Molecular Diversity
https://doi.org/10.1007/s11030-022-10422-8

ORIGINAL ARTICLE

Cytotoxic effect, enzyme inhibition, and in silico studies of some novel *N*-substituted sulfonyl amides incorporating 1,3,4-oxadiazol structural motif

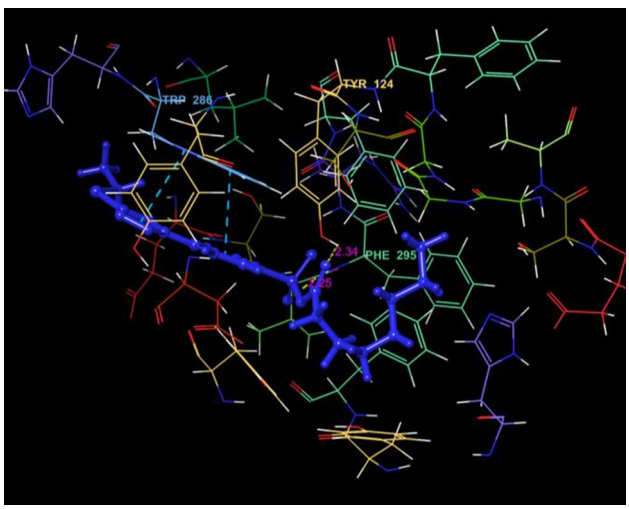
Özcan Güleç[1] · Cüneyt Türkeş[2] · Mustafa Arslan[1] · Yeliz Demir[3] · Yeşim Yeni[4] · Ahmet Hacımüftüoğlu[4] · Ergün Ereminsoy[5] · Ömer İrfan Küfrevioğlu[5] · Şükrü Beydemir[6,7]

Received: 3 November 2021 / Accepted: 21 March 2022
© The Author(s), under exclusive licence to Springer Nature Switzerland AG 2022

Abstract

The acetylcholinesterase and carbonic anhydrase inhibitors (AChEIs and *h*CAIs) remain key therapeutic agents for many bioactivities such as anti-Alzheimer and antiobesity antiepileptic, anticancer, antiinfective, antiglaucoma, and diuretic effects. Here, it has been attempted to discover novel multi-target AChEIs and *h*CAIs that are highly potent, orally bioavailable, may be brain penetrant, and have higher effectiveness at lower doses than tacrine and acetazolamide. After detailed investigations both in vitro and in silico, novel *N*-substituted sulfonyl amide derivatives (**6a–j**) were determined to be highly potent inhibitors for AChE and *h*CAs (K_Is are in the range of 23.11–52.49 nM, 18.66–59.62 nM, and 9.33–120.80 nM for AChE, *h*CA I, and *h*CA II, respectively). Moreover, according to the cytotoxic effect studies, such as the ADME-Tox, cortex neuron cells, and neuroblastoma SH-SY5Y cell line, compounds **6a**, **6d**, and **6h**, which are the most potent representative versus the target enzymes, were identified as orally bioavailable, highly selective, and brain preferentially distributed AChEIs and *h*CAIs. The docking studies revealed precise binding modes between **6a**, **6d**, and **6h** and *h*CA II, *h*CA I, and AChE, respectively. The results presented here might provide a solid basis for further investigation into more potent AChEIs and *h*CAIs.

Graphical abstract



Keywords 1,3,4-oxadiazol · Acetylcholinesterase · Carbonic anhydrase · In silico study · *N*-substituted sulfonyl amide

Extended author information available on the last page of the article

Published online: 09 April 2022

Introduction

Heterocyclic compounds play an essential role in medicinal chemistry. These agents are present in various drugs, most vitamins, many natural products, biomolecules, and biologically active compounds [1–7]. Oxadiazoles, an essential family of this class, have significant biological activities, such as analgesic, anti-inflammatory, anticonvulsive, antiemetic, fungicidal, diuretic, muscle relaxant, and antioxidant activity [8–10]. Oxadiazoles have different isomers. Among them, 1,3,4-oxadiazoles have become a significant construction motif for developing new drugs and have been determined to be more effective than other isomers in terms of biological activity. Compounds containing 1,3,4-oxadiazole cores, depending on the group of which it is a member, have a widespread biological activity spectrum, including antibacterial, antiviral, anticancer, antifungal, antihypertensive, analgesic, anticonvulsant, anti-inflammatory, and antidiabetic [11]. Due to this broad range of biological activities, the oxadiazole ring is used in various chemical reactions as a core part of a molecule. Moreover, many 1,3,4-oxadiazole motif-containing compounds are widely used in clinical medicine and drugs available in the market. For example, raltegravir, zibotentan, furamizole, and tiodazosin may be exhibited as antiretroviral [12], anticancer [13], antibacterial [14], and antihypertensive agents [15], respectively (Scheme S1).

Sulfonamides, which have strong pharmacological effects such as anticancer, antitumor, protease inhibitor, antibacterial, antifungal, antiprotozoal, anti-inflammatory, and anticonvulsants, have been used as medicines for nearly 100 years [16–21]. Since the molecular structure of sulfonyl amides is similar to the structure of the *p*-aminobenzoic acid being synthesized in our body, it interferes with the reactions controlled by this agent and affects the functioning of the metabolism [22, 23]. The more acidic character of the hydrogens on the nitrogen of the *N*-substituted sulfonyl amides in this class causes it to form stronger hydrogen bonds and thus increase its activity [24–29] (Scheme S2).

Alzheimer's disease (AD) is an age-related, complex, and multifactorial, chronic neurodegenerative disease which accounts for most cases of dementia. AD usually leads to cognitive dysfunction accompanied by some behaviors such as difficulty performing familiar tasks, memory loss, problems with language, anxiety, and depression. Many factors have been associated with AD development, and different hypotheses have been proposed, such as the cholinergic hypothesis, tau hypothesis, amyloid hypothesis, oxidative stress, and neuroinflammation. Although many potential drugs targeting these hypotheses have been tested to treat AD, there is no definitive cure. Acetylcholinesterase (AChE; EC 3.1.1.7) is currently one of the only well-validated molecular targets for AD [30, 31]. The AChE inhibitors (AChEIs) used in this direction decrease the hydrolysis of acetylcholine (ACh) into acetate and choline (Ch) and, with this, raise the ACh levels at the synaptic cleft that may stimulate cholinergic receptors and further promote memory function [32–34]. For example, AChE inhibitors such as tacrine, galantamine, rivastigmine, and donepezil remain the leading choice for treating AD today [35].

Carbonic anhydrases (CAs; EC 4.2.1.1) [36] are zinc metalloenzymes [37] that activate the reversible reaction of bicarbonate ions and carbon dioxide in eukaryotes and prokaryotes [38]. CAs are contained in many crucial biosynthetic reactions, such as glucogenesis, lipogenesis, and ureagenesis. Moreover, they are also involved in numerous physiological processes like acid–base balance, electrolyte secretion, calcification, and transport of carbon dioxide and bicarbonate between tissues [39, 40]. *h*CA activators and/or inhibitors (*h*CAIs) display many bioactivities containing anti-Alzheimer, antiobesity, antiepileptic, anticancer, antiinfective, antiglaucoma, and diuretic effects [41]. Therefore, *h*CA I (expressed in erythrocytes) and *h*CA II (expressed in testis, bone osteoclasts, brain, gastrointestinal tract, kidney, erythrocytes, eye, gastrointestinal tract, lung) among the isoenzymes in this class are the most studied ones.

In light of all this literature information, our current efforts were to design novel multi-target AChEIs and *h*CAIs, mainly aiming to decrease administration dose within the safety limits of commercially available drugs. In this direction, a novel series *N*-substituted sulfonyl amide derivative (**6a–j**) were designed, synthesized, characterized, and investigated the biological activities of these compounds on mentioned above target enzymes by this strategy. Because AChEIs generally have high cytotoxicity, the possibility that they may counteract their application as central nervous system-targeting therapeutics also has been considered. Therefore, this study also was investigated cytotoxicity and neurotoxicity profiles of compounds (**6a**, **6d**, and **6h**) being the most potent representative versus the enzymes mentioned above on the cortex neuron cells and neuroblastoma SH-SY5Y cell line. Additionally, in silico studies were performed to assess those inhibitors' inhibition mechanisms against AChE and *h*CAs.

Experimental

General procedure for the preparation of the compounds

Melting points were determined by a Yanagimoto micro-melting point apparatus and are uncorrected. IR spectra were

acquired on a SHIMADZU Prestige-21 (200 VCE) spectrometer. ^{1}H and ^{13}C NMR spectra were acquired at VARIAN Infinity Plus in 300 and 75 Hz, respectively. ^{1}H and ^{13}C chemical shifts are referenced to the internal deuterated solvent. The elemental analysis was carried out with a Leco CHNS-932 instrument. All chemicals were purchased from Sigma-Aldrich.

Ethyl 4-(aminosulfonyl)benzoate (2)

4-Sulfamoylbenzoic acid (10 mmol) was refluxed for 24 h in 50 mL of ethanol and 1.0 mL of sulfuric acid was used as a catalyst. At the end of the reaction, the solvent was evaporated and the obtained product was washed with cold water and dried.

4-sulfonylamidebenzohydrazide (3)

Ethyl-4-(aminosulfonyl)benzoate (10 mmol) and hydrazine hydrate (25 mmol) in ethanol were refluxed for 24 h at 70 °C. The reaction mixture was cooled to room temperature and the solid was filtered then washed with water and dried.

4-(5-thioxo-4,5-dihydro-1,3,4-oxadiazol-2-yl) benzenesulfonamide (4)

Carbon sulfur (2.5 mmol) and 4-sulfonylamidebenzohydrazide (**3**) (1 mmol) were dissolved in DMF (6 mL) and K_2CO_3 (1 mmol) was added to the mixture. Then, it was stirred for 12 h at room temperature. After the reaction was completed, the mixture was cooled to room temperature and poured into ice cold water. It was then filtered, dried, and crystallized.

4-(5-(ethylthio)-1,3,4-oxadiazol-2-yl)benzenesulfonamide (5)

Iodoethane (1.2 mmol) and 4-(5-thioxo-4,5-dihydro-1,3,4-oxadiazol-2-yl)benzenesulfonamide (1 mmol) were dissolved in DMF (6 mL) and K_2CO_3 (1 mmol) was added to the mixture, then, stirred for 12 h at room temperature. After the reaction was completed. The mixture was cooled to room temperature and poured into ice cold water. It was then filtered, dried, and crystallized.

N-substituted ((ethylthio-1,3,4-oxadiazol-2-yl)phenyl) sulfonyl amide derivatives (6a–j)

Acylhalide derivatives (1.2 mmol) and 4-(5-thioxo-4,5-dihydro-1,3,4-oxadiazol-2-yl)benzenesulfonamide (1 mmol) were dissolved in pyridine (5 mL). Then, it was heated for 12 h at 60 °C. After the reaction was completed, the mixture was cooled to room temperature and poured into ice cold water. It was then filtered, dried, and crystallized from acetone. The prepared compounds shown in Scheme 1 were characterized by ^{1}H NMR, ^{13}C NMR, IR, and elemental analysis.

N-([4-(5-(ethylthio)-1,3,4-oxadiazol-2-yl)phenyl]sulfonyl) benzamide (6a)

Yield 75%, m.p. 178 °C. IR (ν_{max}, cm^{-1}): 3666 (N–H), 1683 (C=O), 1458 and 1386 (C–H), 1255 and 1168 (S=O). ^{1}H NMR (300 MHz, DMSO-d_6, ppm): 8.21 (2H, d,=CH), 8,16 (2H, d,=CH), 7,87 (2H, d,=CH), 7,64 (1H, m,=CH), 7,51 (2H, m,=CH), 3.40 (2H, m, $–CH_2$) 1.45 (3H, t, $–CH_3$). ^{13}C NMR (75 MHz, DMSO-d_6, ppm): 170.1, 165.7, 164.2, 149.7, 147.3, 134.3, 131.8, 129.4, 129.1, 127.7, 27.4, 15.5. Anal. calcd. for $C_{17}H_{15}N_3O_4S_2$: C, 52.43; H, 3.88; N, 10.79; O, 16.43; S, 16.47; found: C, 52.47; H, 3.92; N, 10.83; O, 16.55; S, 16.54.

N-([4-(5-(ethylthio)-1,3,4-oxadiazol-2-yl)phenyl] sulfonyl)-4-methylbenzamide (6b)

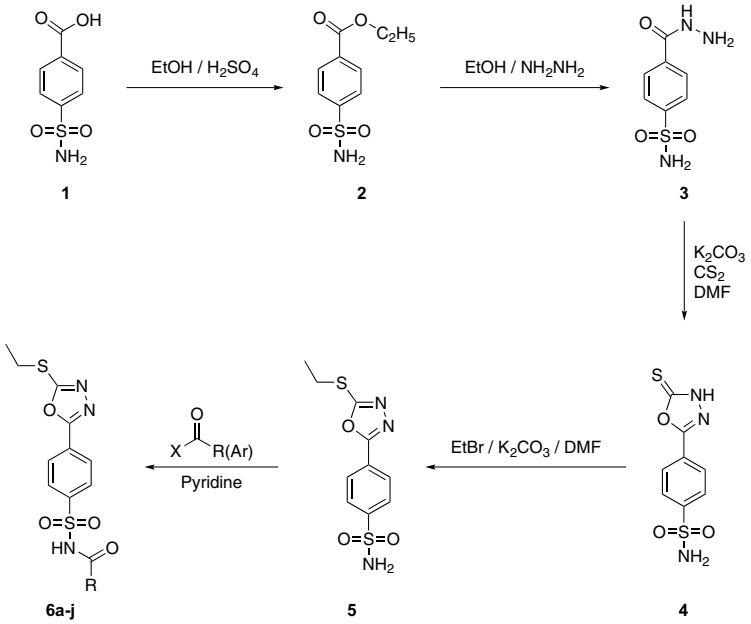
Yield 80%, m.p. 191 °C. IR (ν_{max}, cm^{-1}): 3678 (N–H), 1732 (C=O), 1452 and 1388 (C–H), 1171 and 1068 (S=O). ^{1}H NMR (300 MHz, DMSO-d_6, ppm): 8.25 (2H, d,=CH), 8,21 (2H, d,=CH), 7,82 (2H, d,=CH), 7,31 (2H, d,=CH), 3.37 (2H, m, $–CH_2$), 2.35 (3H, s, $–CH_3$), 1.43 (3H, t, $–CH_3$). ^{13}C NMR (75 MHz, DMSO-d_6, ppm): 171.2, 165.5, 164.6, 144.6, 142.5, 129.8, 129.4, 129.2, 129.0, 127.7, 27.4, 21.8, 15.5. Anal. calcd. for $C_{18}H_{17}N_3O_4S_2$: C, 53.58; H, 4.25; N, 10.41; O, 15.86; S, 15.89; found: C, 53.61; H, 4.33; N, 10.50; O, 15.99; S, 15.94.

N-([4-(5-(ethylthio)-1,3,4-oxadiazol-2-yl)phenyl] sulfonamido)-2-oxoethyl acetate (6c)

Yield 84%, m.p. 209 °C. IR (ν_{max}, cm^{-1}): 3672 (N–H), 1738 (C=O), 1451 and 1382 (C–H), 1230 and 1190 (S=O). ^{1}H NMR (300 MHz, DMSO-d_6, ppm): 8.23 (2H, d,=CH), 8,09 (2H, d,=CH), 4.55 (2H, s, $–CH_3$), 3.38 (2H, m, $–CH_2$), 2.00 (3H, s, $–CH_3$), 1.46 (3H, t, $–CH_3$). ^{13}C NMR (75 MHz, DMSO-d_6, ppm): 171.4, 166.9, 164.5, 155.3, 129.6, 128.4, 127.7, 126.0, 64.7, 27.4, 21.0, 15.3. Anal. calcd. for $C_{14}H_{15}N_3O_6S_2$: C, 43.63; H, 3.92; N, 10.90; O, 24.91; S, 16.64; found: C, 43.74; H, 3.95; N, 10.96; O, 24.99; S, 16.70.

N-([4-(5-(ethylthio)-1,3,4-oxadiazol-2-yl)phenyl]sulfonyl) butyramide (6d)

Yield 72%, m.p. 142 °C. IR (ν_{max}, cm^{-1}): 3675 (N–H), 1708 (C=O), 1455 and 1385 (C–H), 1113 and 1106 (S=O). ^{1}H NMR (300 MHz, DMSO-d_6, ppm): 8.20 (2H, d,=CH), 8,08



Compound ID	R
6a	phenyl
6b	tolyl
6c	acetoxymethyl
6d	propyl
6e	butyl
6f	pentyl
6g	hexyl
6h	heptyl
6i	octyl
6j	undecanolyl

Scheme 1 Synthesis of the novel *N*-substituted sulfonyl amide derivatives (**6a**–**j**)

(2H, d,=CH), 3.33 (2H, m, $-CH_2$), 2.51 (2H, m, $-CH_2$), 2.20 (2H, m, $-CH_2$), 1.44 (3H, t, $-CH_3$), 0.75 (3H, t, $-CH_3$). ^{13}C NMR (75 MHz, DMSO-d_6, ppm): 177.1, 165.5, 160.5, 142.7, 129.2, 127.5, 119.2, 38.1, 27.6, 18.4, 15.5, 13.8. Anal. calcd. for $C_{14}H_{17}N_3O_4S_2$: C, 47.31; H, 4.82; N, 11.82; O, 18.01; S, 18.04; found: C, 47.35; H, 4.87; N, 11.86; O, 18.06; S, 18.10.

N-([4-(5-(ethylthio)-1,3,4-oxadiazol-2-yl)phenyl]sulfonyl) pentanamide (6e)

Yield 76%, m.p. 140 °C. IR (ν_{max}, cm^{-1}): 3662 (N–H), 1712 (C=O), 1452 and 1389 (C–H), 1168 and 1071 (S=O). ^{1}H NMR (300 MHz, DMSO-d_6, ppm): 8.23 (2H, d,=CH), 8,09 (2H, d,=CH), 3.36 (2H, m, $-CH_2$), 2.23 (2H, t, $-CH_2$), 1.44 (3H, t, $-CH_3$), 1.38 (2H, m, $-CH_2$), 1.16 (2H, m, $-CH_2$), 0.79 (3H, t, $-CH_3$). ^{13}C NMR (75 MHz, DMSO-d_6, ppm): 173.0, 166.1, 164.8, 142.4, 129.6, 128.7, 128.0, 36.0, 27.1, 25.8, 22.2, 16.3, 14.6. Anal. calcd. for $C_{15}H_{19}N_3O_4S_2$: C, 48.76; H, 5.18; N, 11.37; O, 17.32; S, 17.36; found: C, 48.82; H, 5.20; N, 11.42; O, 17.38; S, 17.42.

N-([4-(5-(ethylthio)-1,3,4-oxadiazol-2-yl)phenyl]sulfonyl) hexanamide (6f)

Yield 85%, m.p. 122 °C. IR (ν_{max}, cm^{-1}): 3681 (N–H), 1695 (C=O), 1454 and 1385 (C–H), 1115 and 1071 (S=O). ^{1}H NMR (300 MHz, DMSO-d_6, ppm): 8.23 (2H, d,=CH), 8,11 (2H, d,=CH), 3.40 (2H, m, $-CH_2$), 2.20 (2H, t, $-CH_2$), 1.44 (3H, t, $-CH_3$), 1.38 (2H, m, $-CH_2$), 1.25 (2H, m, $-CH_2$), 1.11 (2H, m, $-CH_2$), 0.78 (3H, t, $-CH_3$). ^{13}CNMR (75 MHz, DMSO-d_6, ppm): 171.8, 166.1, 163.6, 142.1, 129.6, 128.6, 127.4, 34.7, 31.4, 27.5, 24.9, 22.2, 15.6, 14.6. Anal. calcd. for $C_{16}H_{21}N_3O_4S_2$: C, 50.11; H, 5.52; N, 10.96; O, 16.69; S, 16.72; found: C, 50.18; H, 5.57; N, 10.99; O, 16.74; S, 16.75.

N-([4-(5-(ethylthio)-1,3,4-oxadiazol-2-yl)phenyl]sulfonyl) heptanamide (6g)

Yield 74%, m.p. 109 °C. IR (ν_{max}, cm^{-1}): 3669 (N–H), 1714 (C=O), 1453 and 1387 (C–H), 1160 and 1068 (S=O). ^{1}H NMR (300 MHz, DMSO-d_6, ppm): 8.21 (2H, d,=CH), 8,13 (2H, d,=CH), 3.42 (2H, m, –CH_2), 2.21 (2H, t, –CH_2), 1.43 (3H, t, –CH_3), 1.37 (2H, m, –CH_2), 1.23 (2H, m, –CH_2), 1.19 (2H, m, –CH_2), 1.10 (2H, m, –CH_2), 0.79 (3H, t, –CH_3). ^{13}C NMR (75 MHz, DMSO-d_6, ppm): 171.8, 166.1, 163.9, 142.4, 129.2, 128.0, 127.7, 35.9, 31.4, 28.5, 27.4, 24.5, 22.5, 15.5, 14.5. Anal. calcd. for $C_{17}H_{23}N_3O_4S_2$: C, 51.36; H, 5.83; N, 10.57; O, 16.10; S, 16.13; found: C, 51.42; H, 5.86; N, 10.62; O, 16.14; S, 16.15.

N-([4-(5-(ethylthio)-1,3,4-oxadiazol-2-yl)phenyl]sulfonyl) octanamide (6h)

Yield 80%, m.p. 99 °C. IR (ν_{max}, cm^{-1}): 3678 (N–H), 1733 (C=O), 1455 and 1389 (C–H), 1168 and 1071 (S=O). ^{1}H NMR (300 MHz, DMSO-d_6, ppm): 8.22 (2H, d,=CH), 8,08 (2H, d,=CH), 3.36 (2H, m, –CH_2), 2.52 (2H, m, –CH_2), 2.19 (2H, t, –CH_2), 1.42 (3H, t, –CH_3), 1.42 (2H, m, –CH_2), 1.23 (2H, m, –CH_2), 1.13 (2H, m, –CH_2), 0.79 (2H, m, –CH_2), 0.77 (3H, t, –CH_3). ^{13}C NMR (75 MHz, DMSO-d_6, ppm): 172.5, 165.6, 164.8, 142.4, 129.2, 128.0, 127.7, 36.0, 34.33, 31.8, 29.7, 28.9, 24.6, 22.7, 15.5, 14.5. Anal. calcd. for $C_{18}H_{25}N_3O_4S_2$: C, 52.53; H, 6.12; N, 10.21; O, 15.55; S, 15.58; found: C, 52.46; H, 6.18; N, 10.24; O, 15.67; S, 15.61.

N-([4-(5-(ethylthio)-1,3,4-oxadiazol-2-yl)phenyl]sulfonyl) nonanamide (6i)

Yield 60%, m.p. 110 °C. IR (ν_{max}, cm^{-1}): 3662 (N–H), 1739 (C=O), 1458 and 1385 (C–H), 1117 and 1071 (S=O). ^{1}H NMR (300 MHz, DMSO-d_6, ppm): 8.23 (2H, d,=CH), 8,12 (2H, d,=CH), 3.37 (2H, m, –CH_2), 2.21 (2H, m, –CH_2), 1.43 (3H, t, –CH_3), 1.37 (2H, m, –CH_2), 1.34–1.00 (10H, m, –CH_2), 0.85 (3H, t, –CH_3). ^{13}C NMR (75 MHz, DMSO-d_6, ppm): 173.8, 165.9, 164.8, 142.4, 129.2, 128.0, 127.6, 35.7, 33.5, 31.9, 29.2, 28.8, 27.3, 25.1, 22.7, 15.5, 14.5. Anal. calcd. for $C_{19}H_{27}N_3O_4S_2$: C, 53.62; H, 6.39; N, 9.87; O, 15.04; S, 15.07; found: C, 53.69; H, 6.42; N, 9.99; O, 15.12; S, 15.20.

N-([4-(5-(ethylthio)-1,3,4-oxadiazol-2-yl)phenyl]sulfonyl) dodecanamide (6j)

Yield 76%, m.p. 88 °C. IR (ν_{max}, cm^{-1}): 3680 (N–H), 1695 (C=O), 1454 and 1384 (C=N), 1167 and 1068 (S=O). ^{1}H NMR (300 MHz, DMSO-d_6, ppm): 8.22 (2H, d,=CH), 8,09 (2H, d,=CH), 3.38 (2H, m, –CH_2), 2.20 (2H, m, –CH_2), 1.42 (3H, t, –CH_3), 1.37 (2H, m, –CH_2), 1.33–0.98 (16H, m, –CH_2), 0.85 (3H, t, –CH_3). ^{13}C NMR (75 MHz, DMSO-d_6, ppm): 174.2, 166.6, 164.2, 142.7, 129.3, 127.6, 127.3, 36.1, 34.3, 33.5, 32.7, 30.5, 29.4, 28.5, 27.8, 26.4, 25.2, 23.8, 15.9, 14.3. Anal. calcd. for $C_{22}H_{33}N_3O_4S_2$: C, 56.50; H, 7.11; N, 8.99; O, 13.69; S, 13.71; found: C, 56.58; H, 7.16; N, 9.06; O, 13.72; S, 13.83.

Biological studies

AChE and *h*CAs activity assay

In the present work, AChE from *Electrophorus electricus* (Sigma C2888) was purchased from Sigma-Aldrich Chemie GmbH. In vitro effects on AChE activity of the newly synthesized *N*-substituted sulfonyl amides (**6a–j**) incorporating 1,3,4-oxadiazol structural motif and reference compound, THA, were evaluated by the method of Ellman et al. [42, 43]. Analysis results were obtained spectrophotometrically at 412 nm using acetylthiocholine iodide (PubChem CID: 74629, Sigma 01480) as a substrate as in our previous assays [44, 45]. Also, *h*CAs (*h*CA I and II) were purified from human erythrocytes by Sepharose-4B-L-tyrosine-sulfanilamide affinity chromatography. The inhibition effects of these *N*-substituted sulfonyl amide derivatives (**6a–j**) and reference compound, AAZ versus the esterase activity of the *h*CAs were determined by following the change in absorbance at 348 nm according to the assay defined by Verporte et al. [46–48]. *h*CAs activities were measured using 4-nitrophenyl acetate (PubChem CID: 13,243, Sigma N8130). All the measurements were repeated thrice.

AChE and *h*CAs kinetic assay

To investigate the in vitro inhibitory mechanisms of the novel synthesized *N*-substituted sulfonyl amides (**6a–j**) incorporating 1,3,4-oxadiazol structural motif, kinetic studies were made with the variable compound and substrate concentrations, and IC_{50} curves, Michaelis–Menten graphs [49–51], and Lineweaver–Burk curves [52–54] were generated as previously reported by Türkeş et al. [55–57]. Solutions of the novel synthesized all agents (**6a–j**), THA, and AAZ were prepared in dimethyl sulfoxide (PubChem CID: 679, Sigma D8418, DMSO) at an initial concentration of 1 mg/mL. The concentration of DMSO in the final reaction mixture was approx. 1%. IC_{50} and K_I values for these derivatives were computed from the observed data, and the types of inhibition of AChE and hCAs were determined as in our previous studies [58–60]. Analysis of the data and drawing of graphs were realized using GraphPad Prism version 8 for Mac (GraphPad Software, La Jolla California USA). The inhibition constants were calculated by SigmaPlot version 12 for Windows (Systat Software, San Jose California

USA). The fit of enzyme inhibition models was compared using the extra sum-of-squares *F* test and Akaike's corrected information criterion approach. The results were exhibited as mean ± standard error of the mean (95% confidence intervals). Differences between data sets were considered statistically significant when the *p* value was less than 0.05.

Cell-based assay

The cortex neuron cells and neuroblastoma SH-SY5Y cell line was obtained from the Department of Medical Pharmacology, Faculty of Medicine, Atatürk University (Erzurum, Turkey). The cells were cultured in Dulbecco's modified Eagle's medium (Gibco, Grand Island, NY, USA) supplemented with 15% fetal bovine serum, and 1% antibiotic (penicillin, streptomycin, and amphotericin B), in a humidified atmosphere of 95% air and 5% CO_2 at 37 °C, and grown to 80% confluence [61, 62]. Before cell treatment, the complete medium was replaced with a reduced serum medium (i.e., with 2% fetal bovine serum). The novel synthesized *N*-substituted sulfonyl amide derivatives **6a**, **6d**, and **6h**, which are the most potent representative versus the target enzymes, were prepared as stock solutions in DMSO at an initial concentration of 1 mg/mL. The cytotoxicity of these derivatives **6a**, **6d**, and **6h** was compared with standard compound cisplatin. They were administered in four different doses (10, 100, 500, and 1000 µM) in a quadruplicate. After 24 h, on cortex neuron cells and SH-SY5Y cell line treated by seeding in 96-well plates with compounds **6a**, **6d**, and **6h**, the administration was terminated, and the MTT (3-[4,5-dimethylthiazol-2-yl]-2,5-diphenyltetrazolium bromide) cytotoxicity test was performed. After the medium aspirating process of 10 µL, an MTT solution was added to each well. The plates containing the applications were kept for 4 h in an environment containing 5% CO_2 at 37 °C with MTT solution [63]. To dissolve the formazan crystals formed as a result of MTT, 100 µL DMSO was added to each well [64]. To determine the density of formazan crystals, data were obtained by reading plates with a Multiskan Go Microplate Spectrophotometer reader at a wavelength of 570 nm. Additionally, morphological changes occurring in the cortex neuron cells and SH-SY5Y cell line were visualized with an inverted microscope (Leica Microsystems, Wetzlar, Germany). The images obtained were recorded with × 200 magnification of the microscope [65]. GraphPad Prism version 8 for Mac (GraphPad Software, La Jolla California USA) was used for the statistical analyses to assess the results obtained in the study. The One-way ANOVA method was used to analyze the data, and the significance values were compared with the control group. Differences between data sets were considered statistically significant when the *p* value was less than 0.05.

Computational studies

ADME-Tox assay

In silico ADME-Tox assays were computed using Schrödinger Small-Molecule Drug Discovery Suite (Schrödinger Release 2021–1 panels for Mac: Maestro [66], LigPrep [67], QikProp [68, 69]; Schrödinger, LLC, NY, USA) and SwissADME platform for the novel synthesized *N*-substituted sulfonyl amides (**6a–j**) incorporating 1,3,4-oxadiazol structural motif. The ligands (compounds **6a–j** and the reference compounds, THA and AAZ) were firstly sketched using ChemDraw [70] version 19.1 for Mac (PerkinElmer, Inc., Waltham, MA, USA), were prepared by LigPrep, and were lastly evaluated utilizing QikProp in normal processing mode. QikProp properties and prediction ranges for ADME-Tox include: MW (130.0–725.0), Dipole (1.0–12.5), Volume (500.0–2000.0), QPlogPoct (8.0–35.0), QPlogPw (4.0–45.0), QPlogPo/w (–2.0 to 6.5), QPlogS (–6.5 to 0.5), QPPCaco (< 25 poor, great > 500), QPlogBB (–3.0 to 1.2), QPPMDCK (< 25 poor, great > 500), QPlogKp (–8.0 to –1.0), QPlogKhsa (–1.5 to 1.5), HOA (< 25% poor, high > 80%), PSA (7.0–200.0), number of violations of Lipinski's rule of five (max. 4) [71], number of violations of Jorgensen's rule of three (max. 3) [72], and PAINS alert [73].

Molecular docking assay

The potential modes of the binding of for the novel synthesized *N*-substituted sulfonyl amides (**6a–j**) incorporating 1,3,4-oxadiazol structural motif to target proteins (AChE, *h*CA I, and *h*CA II) were investigated with Schrödinger Small-Molecule Drug Discovery Suite 2021–1 for Mac (Schrödinger, LLC, NY, USA), under the Maestro graphical user interface. Other associated panels included Protein Preparation Wizard [74], SiteMap [75], LigPrep [76], Receptor Grid Generation [77], Ligand Docking [78], and Prime MM-GBSA [79]. The crystal structures of AChE [80] (Species: *Homo sapiens*; PDB code 4EY7; Resolution: 2.35 Å; *R*-Values free, work, and observed: 0.211, 0.175, and 0.177, respectively), *h*CA I [81] (Species: *Homo sapiens*; PDB code 6I0L; Resolution: 1.40 Å; *R*-Values free, work, and observed: 0.237, 0.204, and 0.206, respectively), and *h*CA II [82] (Species: *Homo sapiens*; PDB code 5NY3; Resolution: 1.40 Å; *R*-values free, work, and observed: 0.172, 0.156, and 0.157, respectively) were obtained from Protein Data Bank (http://www.rcsb.org/) [83] were applied for in silico molecular docking. The 4EY7, 6I0L, and 5NY3 in the crystal structures were minimized using the Protein Preparation Wizard tool [84] has been used for preparing the protein structure where bond orders were assigned

and hydrogen atoms were added as well as restrained minimization step has also been done using optimized potential liquid simulations 4 (OPLS4) force field [85] at pH 7.4 ± 0.5 [86]. The active sites of theirs were predicted utilizing the SiteMap panel [87]. The ligand-binding sites were calculated using the Receptor Grid Generation tool [88]. LigPrep module was used for preparing all the synthesized *N*-substituted sulfonyl amides (**6a–j**) where bond order and the bond angle were assigned as well as minimization was done using OPLS4 force field [89]. The prepared small molecules were docked into the binding sites of the target enzymes by the Ligand Docking module with Glide extra precision (XP) mode [90–92]. MM-GBSA relative binding free energy computations [93–95] of target proteins (4EY7, 6I0L, and 5NY3) with the agents were carried out using the Prime tool in the VSGB energy model and OPLS4 force field [96, 97].

Results and discussion

Drug design strategy and chemistry

Ethyl 4-(aminosulfonyl)benzoate was prepared from sulfamoylbenzoic acid in ethanol with catalytic amount of sulfuric acid by refluxing for 24 h. The ester group of the ethyl 4-(aminosulfonyl)benzoate was converted to 4-sulfonylamidebenzohydrazide with hydrazine hydrate in ethanol at 70 °C for 24 h. 4-(5-thioxo-4,5-dihydro-1,3,4-oxadiazol-2-yl)benzene sulfonamide was prepared by reacting Carbon disulfur and 4-sulfonylamide benzohydrazide in DMF in the presence of K_2CO_3. 4-(5-(ethylthio)-1,3,4-oxadiazol-2-yl) benzene sulfonamide was synthesized using Iodoethane and the compound **4** in DMF in basic condition. The final targeted compounds **(6a–j)** were prepared by acylhalide derivatives and the compound **5** in pyridine at 60 °C. The prepared compounds **(6a–j)** shown in Scheme 1 were characterized by ^{1}H NMR, ^{13}C NMR, IR, and elemental analysis. From the ^{1}H NMR spectra of the compounds, sulfanilamide NH resonances at very low field due to electron delocalization and the =CH proton peaks on aromatic ring come between 8.05 and 8.25 ppm. The signals of carbonyl and oxadiazole ring are seen at around 170 ppm and 165 ppm, respectively, in the ^{13}C NMR spectra. In the infrared spectra of compounds **6a–j**, it was possible to observe the absorptions around 3660 cm^{-1} and 1700 cm^{-1} relating to N–H and C=O stretchings, respectively. As seen in the literature [98], there are two peaks assigned to S=O as asymmetric and symmetric stretching which are appeared around 1300 and 1100 cm^{-1}, respectively. All spectra and elemental analyses support the structure of the synthesized compounds.

Biological studies

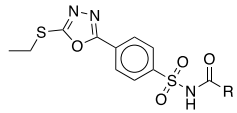
Inhibition study and structure–activity relationship assay

The *h*CAs and AChE inhibitory impact for all herein prepared target *N*-substituted sulfonyl amides (**6a–j**) incorporating 1,3,4-oxadiazol structural motif, as well as the standards, *h*CAI acetazolamide (AAZ; K_Is for *h*CA I and *h*CA II 439.17 ± 9.30 and 98.28 ± 1.69 nM, respectively) and AChEI tacrine (THA; K_Is for AChE 155.29 ± 0.82 nM), were estimated versus the ubiquitous cytosolic *h*CA I, II isoforms, and AChE by the use of the Verpoorte's and Ellman's methods, respectively. Certain structure–activity relationships (SAR) could be drawn from the shown inhibition data in Table 1.

Regarding the *h*CAs inhibitory activities of *N*-substituted sulfonyl amides, all derivatives (**6a–j**) displayed potent inhibitory action against the ubiquitous cytosolic *h*CA I isoform with K_I constants ranging from 18.66 ± 0.21 to 59.62 ± 0.53 nM (Table 1). In particular, *N*-substituted sulfonyl amide **6d** (propyl substituted), **6a** (phenyl substituted), and **6g** (hexyl substituted) exhibited the best *h*CA I inhibitory activity with two-digit nanomolar activities with K_Is equal 18.66 ± 0.21, 21.64 ± 0.25, and 23.01 ± 0.29 nm, respectively. Interestingly, the kinetic value of the compound **6d**, which is the lowest in the series, displayed a 23.5-fold lower K_I when compared to the reference AAZ (K_I = 439.17 ± 9.30 nM). It is worth stressing that replacement of a propyl group (derivative **6d**; K_I = 18.66 ± 0.21 nM) with a tolyl group (derivative **6b**; K_I = 59.62 ± 0.53 nM) resulted in a more than threefold inhibition increase for the cytosolic *h*CA I isoform. On the other hand, it is determined that elongation of the sulfonyl acetamide linker in the butyl tail-bearing compound **6e** (K_I = 47.15 ± 0.36 nM) resulted in an increase in isoform *h*CA I inhibitory activity (derivatives **6f**, **6g**, **6h**, **6i**, and **6j**; with K_Is of 33.10 ± 0.47, 23.01 ± 0.29, 34.61 ± 0.51, 38.40 ± 0.46, and 31.01 ± 0.41 nM, respectively).

Moreover, exploring the inhibitory activity of herein reported *N*-substituted sulfonyl amide derivatives (**6a–j**) versus the physiologically dominant *h*CA II isoform revealed that it was effectively inhibited by sulfonyl amides (**6a–j**) with K_Is spanning in the range 9.33 ± 0.13–120.80 ± 0.34 nM (Table 1). Superiorly, compound **6a** (phenyl substituted) exerted single-digit nanomolar inhibitory activity versus *h*CA II isoform (K_Is = 9.33 ± 0.13 nM), thus resulting in 10.5-fold higher potency when compared to the reference AAZ (K_I = 98.28 ± 1.69 nM), besides, compounds **6b**, **6c**, and **6d** displayed K_I constants close to each other 17.84 ± 0.23, 22.20 ± 0.22, and 23.18 ± 0.26 nM, respectively. Contrariwise, *h*CA II isoform was weakly inhibited by compounds **6h** and **6i** with K_Is of 120.80 ± 0.34 and 112.70 ± 0.36 nM,

Table 1 Inhibition data of AChE and *h*CA I, II isoforms with novel synthesized *N*-substituted sulfonyl amides (**6a–j**) incorporating 1,3,4-oxadiazol structural motif



6a-j

Compound		AChE		*h*CA I		*h*CA II		Selectivity index [a]				
ID	*R*	K_I (nM)	Inhibition type	K_I (nM)	Inhibition type	K_I (nM)	Inhibition type	THA[b]/AChE	AAZ[c]/*h*CA I	AAZ[c]/*h*CA II	*h*CAI/*h*CA II	*h*CA II/*h*CA I
6a	Phenyl	52.49 ± 1.27	Competitive	21.64 ± 0.25	Competitive	9.33 ± 0.13	Competitive	2.96	20.29	10.53	2.32	0.43
6b	Tolyl	47.03 ± 1.71	Competitive	59.62 ± 0.53	Noncompetitive	17.84 ± 0.23	Competitive	3.30	7.37	5.51	3.34	0.30
6c	Acetoxymethyl	47.01 ± 1.95	Competitive	29.62 ± 0.28	Competitive	22.20 ± 0.22	Competitive	3.30	14.83	4.43	1.33	0.75
6d	Propyl	48.38 ± 1.75	Competitive	18.66 ± 0.21	Competitive	23.18 ± 0.26	Competitive	3.21	23.54	4.24	0.81	1.24
6e	Butyl	41.23 ± 0.95	Noncompetitive	47.15 ± 0.36	Competitive	37.24 ± 0.14	Competitive	3.77	9.31	2.64	1.27	0.79
6f	Pentyl	39.34 ± 1.13	Competitive	33.10 ± 0.47	Competitive	29.19 ± 0.10	Competitive	3.95	13.27	3.37	1.13	0.88
6g	Hexyl	49.70 ± 2.13	Competitive	23.01 ± 0.29	Competitive	30.71 ± 0.09	Competitive	3.12	19.09	3.20	0.75	1.33
6h	Heptyl	23.11 ± 0.77	Competitive	34.61 ± 0.51	Competitive	120.80 ± 0.34	Noncompetitive	6.72	12.69	0.81	0.29	3.49
6i	Octyl	47.56 ± 1.75	Competitive	38.40 ± 0.46	Competitive	112.70 ± 0.36	Competitive	3.27	11.44	0.87	0.34	2.93
6j	Undecanoyl	46.70 ± 1.64	Competitive	31.01 ± 0.41	Competitive	29.40 ± 0.13	Competitive	3.33	14.16	3.34	1.05	0.95
THA[c]	–	155.29 ± 0.82	Competitive	–	–	–	–	–	–	–	–	–
AAZ[d]	–	–	–	439.17 ± 9.30	Noncompetitive	98.28 ± 1.69	Noncompetitive	–	–	–	–	–

[a]The K_I rates are indicative of selectivity index: A potent selective inhibitor is characterized by a high-value ratio

[b]Tacrine

[c]Acetazolamide

respectively. It is worth mentioning that replacing the tolyl tail of derivative **6b** ($K_I = 17.84 \pm 0.23$ nM) with a phenyl one, as in compound **6a**, resulted in about twofold enhanced inhibitory potency against *h*CA II isoform ($K_I = 9.33 \pm 0.13$ nM). Furthermore, branching of the sulfonyl acetamide linker and its elongation decreased the *h*CA II inhibitory action for the heptyl tail-bearing derivative **6h**. Moreover, it is worth highlighting that *h*CAIs profiles presented in Table 1 hinted out that compound **6b** demonstrated interesting selectivity versus the ubiquitous cytosolic *h*CA I isoform (selectivity index; $S_I = 3.34$), whereas compound **6h** has shown selectivity against the dominant *h*CA II isoform ($S_I = 3.49$). Hence, further structural modifications are required to optimize the *h*CA II/I selectivity. This selectivity for compounds **6b** and **6h** makes understand them as exciting and promising candidates for further improvement as potential *h*CAIs.

Recently, an increasing number of different *h*CAIs than the sulfonamides and their bioisosteres have been identified. In this context, the study by Sharma et al. [99] reported that two novel series of 1,3,4-oxadiazole benzenesulfonamide hybrids **3** and **4**, having twenty novel compounds, have been designed and synthesized to assess their inhibition potential as *h*CAIs against *h*CA I, II, IX, and XII. They found that potent inhibitory activity versus *h*CA I has been exhibited by derivatives **3g** and **4j**, 3.5-fold of order better than standard drug AAZ and derivative **4j** effectively inhibited glaucoma-associated *h*CA II isoform as well as tumor-associated *h*CA IX isoform. Rutkauskas et al. [100] reported that a series of *N*-aryl-*β*-alanine derivatives and diazobenzenesulfonamides containing aliphatic rings were designed, characterization, synthesized, and their binding to *h*CA I, II, VI, VII, XII, and XIII isoenzymes was studied using the fluorescent thermal shift assay and isothermal titration calorimetry. They determined that 4-substituted diazobenzenesulfonamides were more potent *h*CA binders than *N*-aryl-*β*-alanine derivatives.

The obtained inhibition constants for the AD-related AChE (Table 1) showed that all sulfonyl amides (**6a–j**) were capable of inhibiting this enzyme in the low nanomolar range (K_Is of 23.11 ± 0.77–52.49 ± 1.27 nM). Derivatives **6f** (pentyl substituted) and **6h** (heptyl substituted) emerged as the most potent herein reported AChEI endowed with two-digit nanomolar K_I values equal 39.34 ± 1.13 and 23.11 ± 0.77 nM, respectively (Table 1). In addition, the derivative **6h** showed a K_I value 6.7-fold higher when compared to the reference THA ($K_I = 155.29 \pm 0.82$ nM). Similar to the SAR for inhibition of *h*CA I; replacement of a tolyl group (compound **6b**; $K_I = 47.03 \pm 1.71$ nM) with a heptyl group (compound **6h**; $K_I = 23.11 \pm 0.77$ nM) was advantageous for inhibitory activity versus AChE. Also, elongation of the sulfonyl acetamide linker incorporated in the propyl tail-bearing derivative **6d** was more beneficial for AChE inhibition (compound **6d**; $K_I = 48.38 \pm 1.75$ nM), while the elongation of such linker resulted in about twofold increased activity versus AChE (compound **6h**; $K_I = 23.11 \pm 0.77$ nM).

Cell-based assay

Because the cortex neuron cells and neuroblastoma SH-SY5Y cell line express one or more neurofilament proteins, specific norepinephrine uptake, and neuronal marker enzyme activity, since the early 1980s, it is commonly employed in experimental neurological studies, including metabolism, function, and neuronal differentiation analysis, connected to neuroprotection, neurotoxicity, neuroadaptive, and neurodegenerative processes [101]. Thus, to gain further insight into the therapeutic potential for the treatment for AD of these selected novel synthesized *N*-substituted sulfonyl amide derivatives **6a**, **6d**, and **6h** incorporating 1,3,4-oxadiazol structural motif, which are the most potent representative versus the target enzymes, their cell viability, and proliferation activities were determined using the cortex neuron cells and neuroblastoma SH-SY5Y cell line. The colorimetric MTT assay (3-[4,5-dimethylthiazol-2-yl]-2,5-diphenyltetrazolium bromide) was carried to examine the potential cytotoxic effects of these agents. Images of cortex neuron cells and SH-SY5Y cell line obtained by inverted microscope are given in Fig. 1, respectively. The derivatives **6a**, **6d**, and **6h** evaluated in our study caused a decrease in cell viability after 24 h of incubation, depending on the dose (IC_{50}s = 0.95, 0.88, 0.82, and 0.64 μM for **6a**, 0.99, 0.93, 0.87, and 0.74 μM for **6d**, and 0.98, 0.92, 0.65, and 0.58 μM for **6h**, in four different doses, 10, 100, 500, and 1000 μM, respectively). Moreover, they have been determined to display a propensity for high cell viability and neuroprotection at low concentrations (at 10 and 100 μM). However, these compounds showed cytotoxicities on the cortex neuron cells and neuroblastoma SH-SY5Y cells in a concentration-dependent manner, while *N*-substituted sulfonyl amide derivatives **6a**, **6d**, and **6h** were found as non-toxic agents at their effective concentrations on target enzymes (AChE and *h*CAs) (Figs. 2 and 3). Finally, when examining the information obtained in this study, **6a**, **6d**, and **6h** compounds can be considered promising precursors for new design and development of therapeutics against AD. As a result, these agents exhibit that they have AChE inhibitory activity, which supports their use to treat neurological disorders.

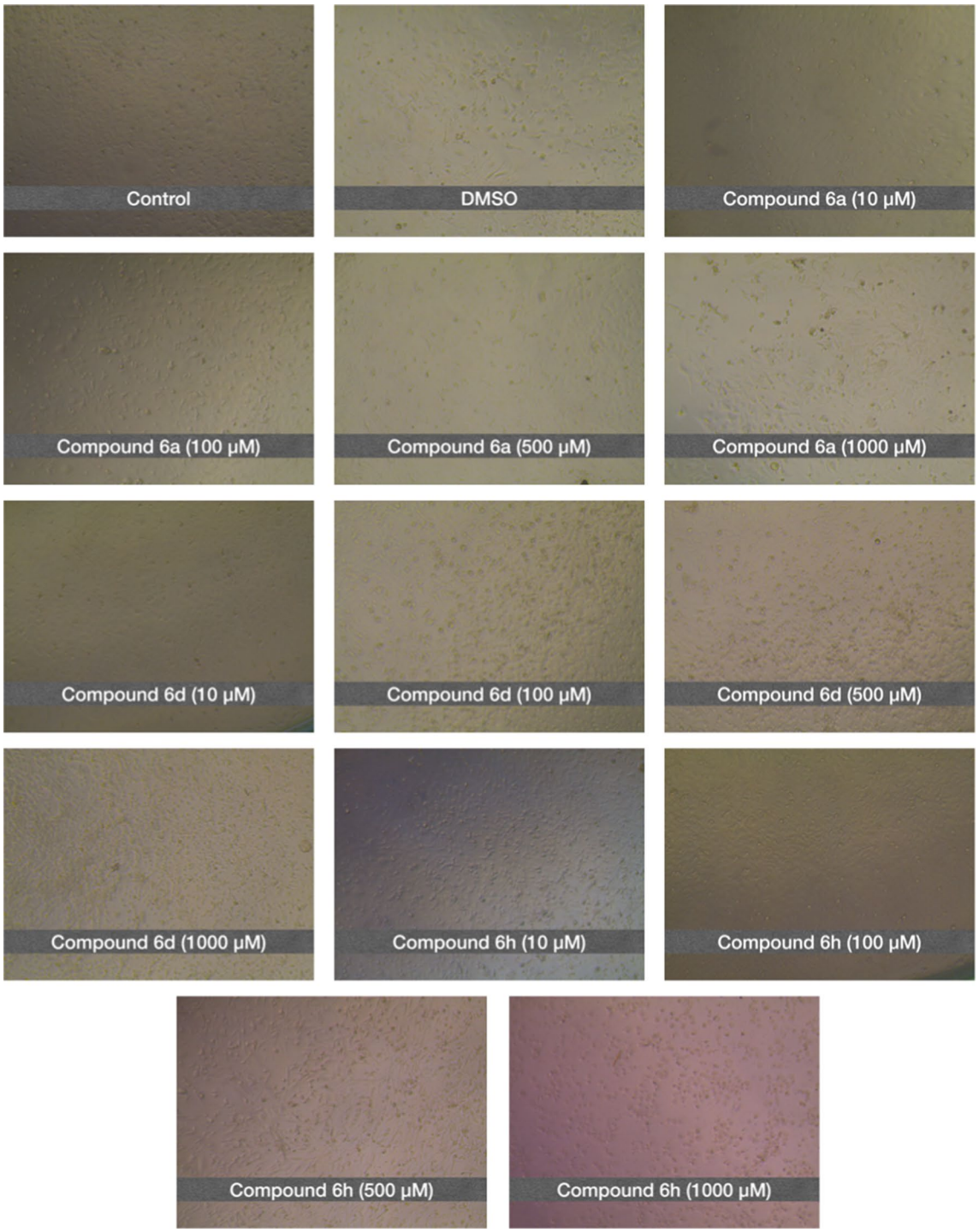


Fig. 1 Inverted microscope images of compounds **6a**, **6d**, and **6h** on cell viability in cortex neuron cells

Computational studies

ADME-Tox assay

All novel *N*-substituted sulfonyl amides (**6a–j**) incorporating 1,3,4-oxadiazol structural motif were evaluated in silico using the ADME-Tox prediction program QikProp, and SwissADME platform, and the findings are reported in Table 2. All properties computed were satisfactory pharmacodynamic and pharmacokinetic properties for the novel synthesized *N*-substituted sulfonyl amide derivatives (**6a–j**). Additionally, diagrams showing "drug-likeness"

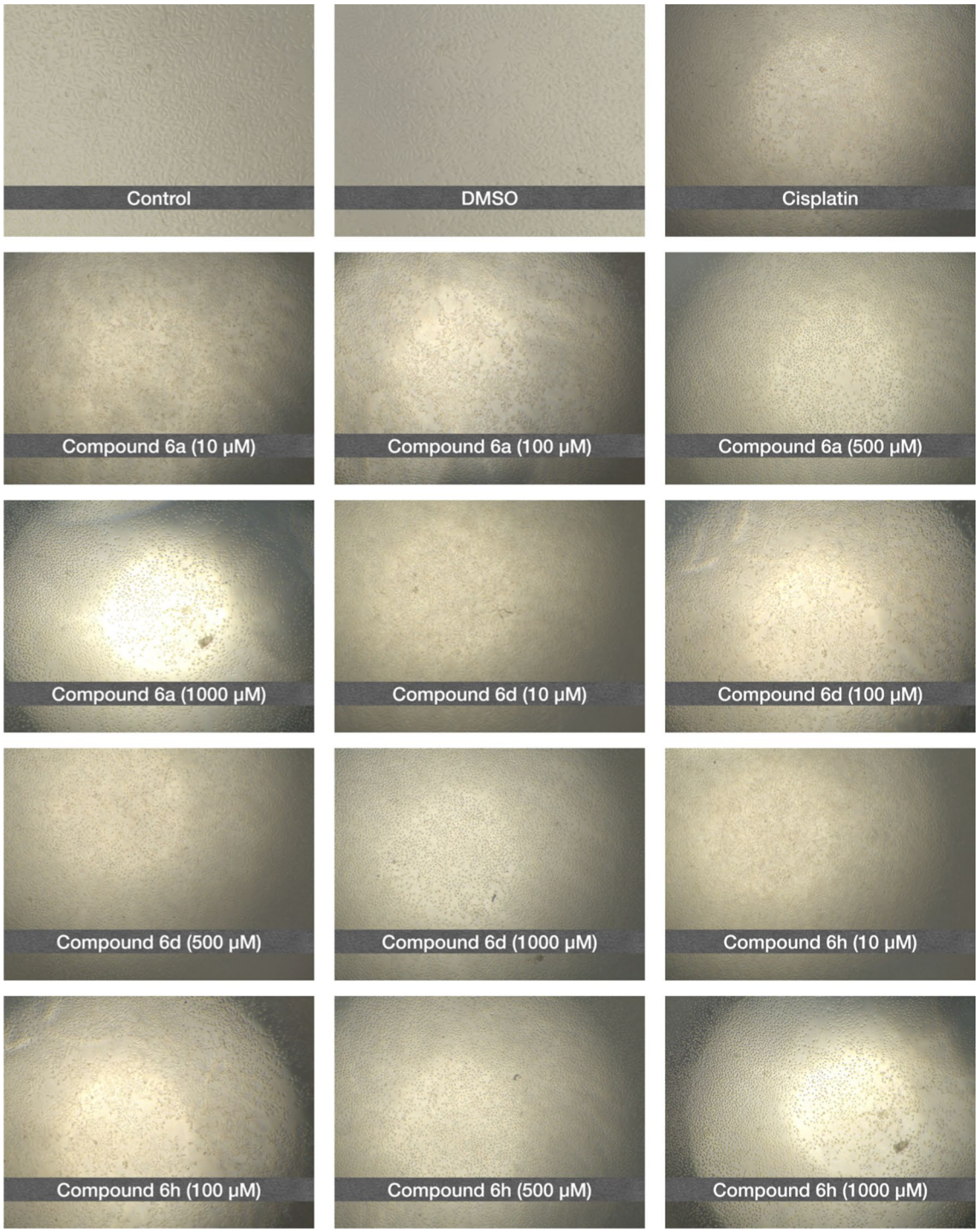


Fig. 2 Morphological changes of SH-SY5Y after 24 h of incubation with concentrations (10–1000 μM) of compounds **6a**, **6d**, and **6h** the results presented are from that were carried out and photographed microscopically

descriptors for **6a**, **6d**, and **6h** agents, which are the most active derivatives in this series, are given in Fig. S1. Only one (compound **6j**) of all *N*-substituted sulfonyl amide derivatives (**6a–j**) were displayed one Lipinski's rule violation, and five agents (compounds **6b** and **6g–j**) showed only one Jorgensen's rule violation. Namely, computed in silico ADME-Tox properties confirmed newly synthesized these sulfonyl amides (**6a–j**) as hit agents displaying suitable drug-like properties.

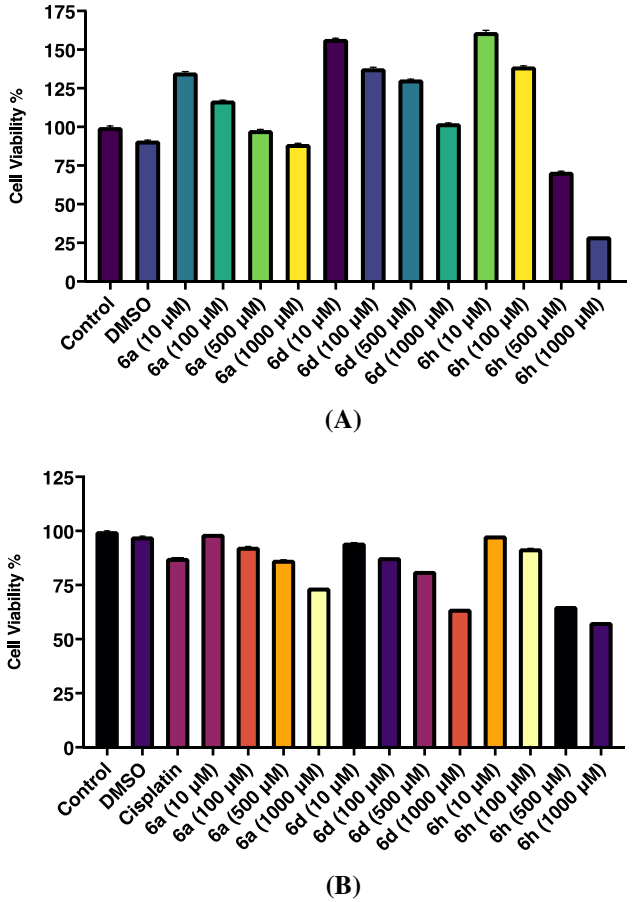


Fig. 3 Cytotoxicity study of compounds **6a**, **6d**, and **6h** on SH-SY5Y cells. The treatment of SH-SY5Y cells was performed with these groups at concentrations varying between 10 and 1000 µM. Every bar represents the mean ± standard error of the mean (95% confidence intervals) of three separate tests. **A** Viability rates for cortex neuron cells and **B** viability rates for neuroblastoma SH-SY5Y cell line

Molecular docking assay

To gain major insights into the causes of SARs researched for novel synthesized *N*-substituted sulfonyl amides (**6a–j**) incorporating 1,3,4-oxadiazol structural motif, molecular docking studies were performed. Firstly, for the redocking computes, the native ligands, E20 (1-Benzyl-4-[(5,6-dimethoxy-1-indanon-2-yl)methyl]piperidine), GZH (1-[4-chloranyl-3-(trifluoromethyl)phenyl]-3-[2-(4-sulfamoylphenyl)ethyl]urea), and 9E8 (1-(4-Chlorophenyl)-3-[2-(4-sulfamoylphenyl)ethyl]urea), in the receptors' binding sites (AChE, PDB code 4EY7; *h*CA I, PDB code 6I0L; and *h*CA II, PDB code 5NY3, respectively) were used. The docked poses of E20, GZH, and 9E8 overlapped with the poses in the X-ray crystal structures of the AChE, *h*CA I, and *h*CA II at a root mean square deviation (RMSD) values of 0.62, 1.51, and 1.20 Å, respectively (Fig. 4). These redocking assays were instrumental for selecting the best model structures that could host all the newly synthesized AChE, *h*CA I, and *h*CA II inhibitors, namely, novel *N*-substituted sulfonyl amide derivatives (**6a–j**). After that, the constructed binding model was used to perform docking calculations of the most potent AChE, *h*CA I, and *h*CA II inhibitors, compounds **6h**, **6d**, and **6a**, respectively, in this series (**6a–j**) employing the Ligand Docking panel.

The predicted binding mode (docking score of − 7.34 kcal/mol and MM-GBSA value of − 49.23 kcal/mol) between compound **6h** and AChE showed that an H-bond interaction was generated between the oxygen atom of the sulfonamide moiety and Phe295 residue (distance of 2.25 Å). Also, Tyr124 (distance of 2.34 Å) made an H-bond with the carboxy group. However, both benzyl ring and oxadiazole-moiety stacked against Trp286 in the peripheral anionic site. Furthermore, hydrophobic interactions were monitored between derivative **6h** and Tyr72, Ala204, Leu289, Val294, Phe297, Tyr337, Phe338, and Tyr341 residues (Fig. 5). A docking score of − 4.10 kcal/mol and MM-GBSA value of − 11.96 kcal/mol indicated that compound **6d** is a tight binder for *h*CA I. A further look into the structural properties revealed agent **6d** coordinated to the Zn(II) ion employing the deprotonated sulfonamide moiety, which in turn is involved in an H-bond interaction with the amide nitrogen of Thr200 (distance of 2.28 Å); further, the oxadiazole-moiety of derivative **6d** displayed the strong H-bond involvement with Gln92 residue (distance of 2.60 Å). Moreover, it was exhibited that residues Phe91, Ala121, Leu131, Ala132, Ala135, Leu141, Val143, Leu198, Pro202, Val207, and Trp209 play significant roles in the binding of agent **6d** with *h*CA I (Fig. 6). One oxygen atom of the sulfonamide moiety of compound **6a** (docking score of − 4.58 kcal/mol and MM-GBSA value of − 26.13 kcal/mol) formed an H-bond with the Asn62 (distance of 2.76 Å), while the other oxygen atom made two H-bonds with the Asn67 and Gln92 (distances of 2.48 and 1.91 Å, respectively) from the binding site residues of *h*CA II. Also, the oxadiazole-moiety displayed $\pi - \pi$ stacking interaction with Trp5 and His64. Additionally, compound **6a** interacted with the hydrophobic pocket formed by Ala65, Val121, Leu141, Val143, Leu198, Pro201, Pro202, Val207, and Trp209, in the active site (Fig. 7).

Table 2 ADME-Tox-related parameters of novel synthesized *N*-substituted sulfonyl amides (**6a–j**) and standard inhibitors tacrine (THA), and acetazolamide (AAZ)

Principal descriptors	6a	6b	6c	6d	6e	6f	6g	6h	6i	6j	THA	AAZ	Standard range
MW	389.44	403.47	385.41	355.43	369.45	383.48	397.51	411.53	425.56	467.64	198.27	222.24	130.0–725.0
Dipole	10.28	8.29	7.53	10.66	8.49	7.85	11.66	10.28	10.77	10.60	4.22	10.75	1.0–12.5
Volume	1173.83	1231.90	1166.05	1121.54	1182.85	1237.73	1282.52	1352.00	1426.62	1603.47	710.28	634.45	500.0–2000.0
QPlogPoct	20.62	20.65	20.04	18.82	18.83	19.17	20.22	20.59	21.34	22.81	10.75	17.57	8.0–35.0
QPlogPw	12.63	12.31	13.56	11.08	10.95	10.76	10.47	10.33	10.42	9.97	6.38	15.15	4.0–45.0
QPlogPo/w	2.82	3.12	1.37	2.26	2.64	2.95	3.31	3.68	4.26	5.36	2.59	−1.75	−2.0–6.5
QPlogS	−5.33	−5.86	−4.68	−4.87	−5.30	−5.54	−5.79	−6.03	−7.12	−8.29	−3.14	−1.55	−6.5–0.5
QPPCaco	208.55	212.48	71.86	204.55	203.17	191.94	243.56	208.35	271.45	263.90	2.931.42	36.88	< 25 poor, great > 500
QPlogBB	−1.54	−1.58	−2.27	−1.64	−1.75	−1.85	−1.81	−1.94	−2.07	−2.37	0.37	−1.74	−3.0–1.2
QPPMDCK	154.30	157.85	48.88	150.99	149.90	141.32	186.65	154.11	205.18	199.23	1.582.00	24.13	< 25 poor, great > 500
QPlogKp	−3.11	−3.30	−4.53	−3.70	−3.61	−3.58	−3.31	−3.36	−2.92	−2.67	−1.78	−5.90	−8.0–1.0
QPlogKhsa	0.97	0.25	−0.39	−0.85	0.27	0.13	0.20	0.35	0.49	0.84	0.72	−0.97	−1.5–1.5
HOA	84.96	86.85	68.18	81.54	83.68	85.10	89.02	90.02	95.43	88.71	100.00	44.77	< 25% poor, high > 80%
PSA	110.34	110.37	151.43	111.88	111.91	111.58	109.39	110.49	111.60	111.67	34.21	134.97	7.0–200.0
Rule of Five	0	0	0	0	0	0	0	0	0	1	0	0	max. 4
Rule of Three	0	1	0	0	0	0	1	1	1	1	0	0	max. 3
PAINS	0	0	0	0	0	0	0	0	0	0	0	0	–

Various computational pharmacodynamic and pharmacokinetic parameters of synthesized compounds in this research were predicted such as molecular weight of the compound (MW), computed dipole moment of the compound (dipole), total solvent-accessible volume in cubic angstroms using a probe with a 1.4 Å radius (volume), octanol/gas partition coefficient (QPlogPoct), water/gas partition coefficient (QPlogPw), octanol/water partition coefficient (QPlogPo/w), aqueous solubility (QPlogS), apparent Caco-2 cell permeability in nm/sec (QPPCaco), brain/blood partition coefficient (QPlogBB), apparent MDCK cell permeability in nm/sec (QPPMDCK), skin permeability (QPlogKp), prediction of binding to human serum albumin (QPlogKhsa), human oral absorption (HOA), van der Waals surface area of polar nitrogen and oxygen atoms (PSA), number of violations of Lipinski's rule of five, number of violations of Jorgensen's rule of three, and pan-assay interference compounds (PAINS) alert

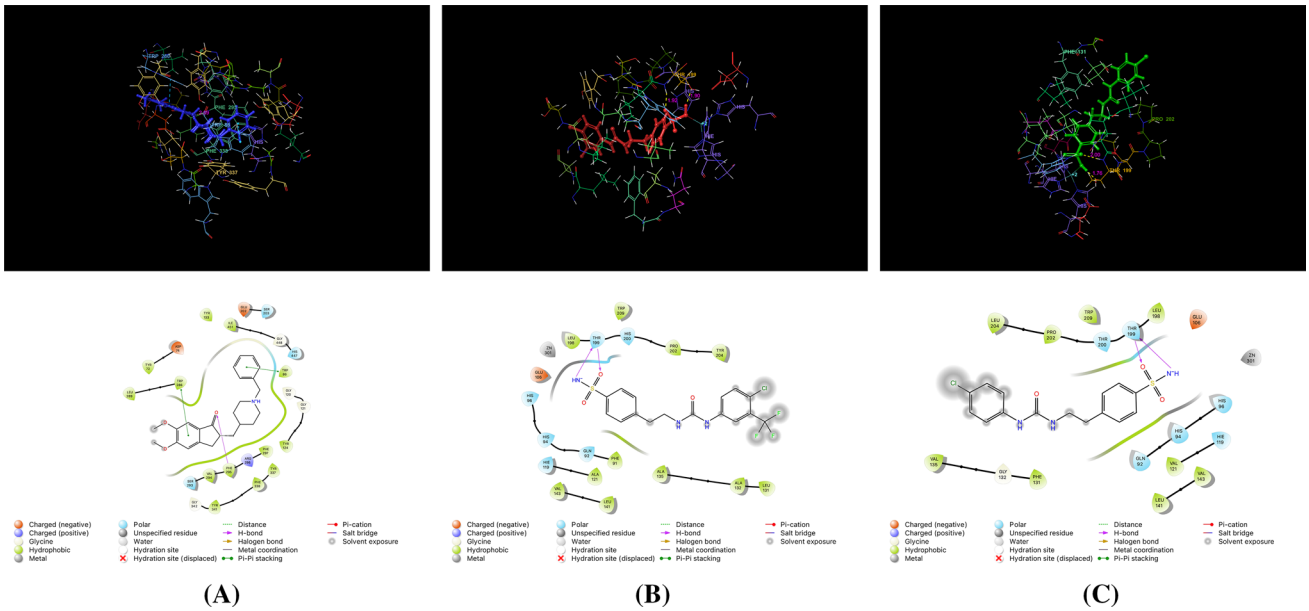
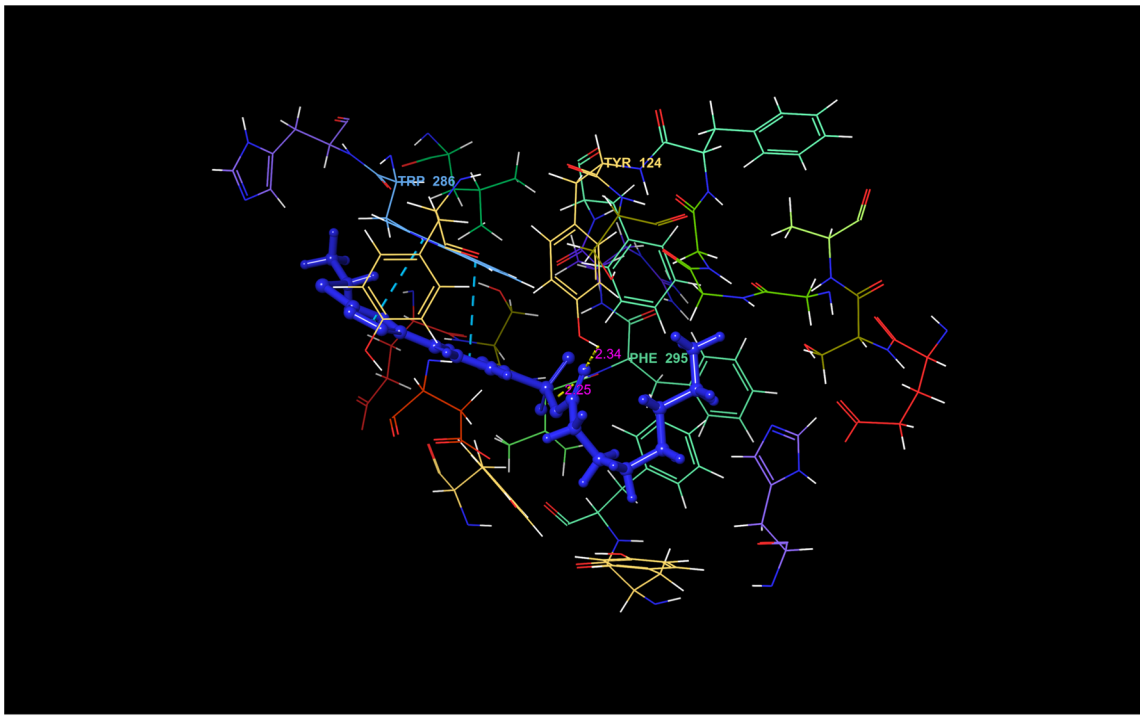


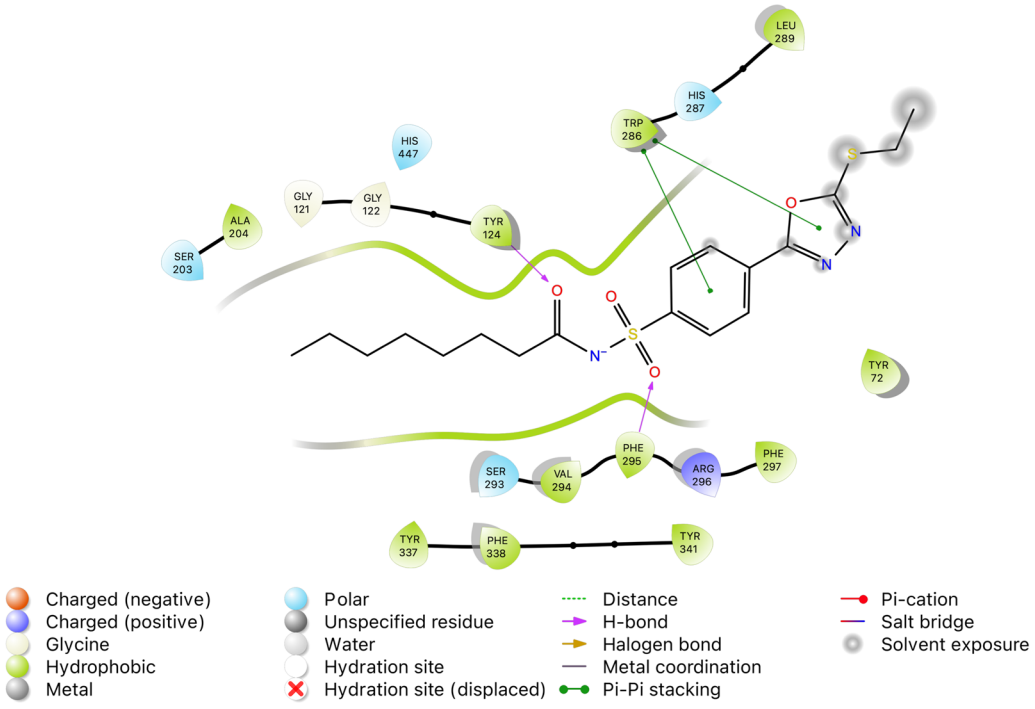
Fig. 4 3D interactions and 2D docking poses of the native ligands **A** E20 ($C_{24}H_{29}NO_3$: 1-benzyl-4-[(5,6-dimethoxy-1-indanon-2-yl) methyl]piperidine) with the key amino acids within the active site of AChE (PDB iD: 4EY7), **B** GZH ($C_{16}H_{15}ClF_3N_3O_3S$: 1-[4-chloro-3-(trifluoromethyl)phenyl]-3-[2-(4-sulfamoylphenyl)ethyl]urea) with the key amino acids within the active site of *h*CA I (PDB iD: 6I0L), and **(C)** 9E8 ($C_{15}H_{16}ClN_3O_3S$: 1-(4-chlorophenyl)-3-[2-(4-sulfamoyl-phenyl)ethyl]urea) with the key amino acids within the active site of *h*CA II (PDB iD: 5NY3)

Conclusion

The small safety window of current AChEIs and *h*CAIs has limited their maximum therapeutic application in the therapy of some metabolic disorders, such as AD, epilepsy, cancer, and glaucoma. Here, we have attempted to design desirable novel multi-target AChEIs and *h*CAIs to overcome this deficiency. By this strategy, novel *N*-substituted sulfonyl amide derivatives (**6a–j**) were synthesized, and all of them displayed excellent inhibitory effects against AChE and *h*CAs. As expected, their effective doses were much lower than that of THA and AAZ, and in silico molecular docking studies on the X-ray co-crystal complexes for three highly potent derivatives (**6a**, **6d**, and **6h**) were provided precise binding modes between the individual agents and *h*CA II, *h*CA I, and AChE, respectively. Overall, according to both in silico ADME-Tox and cytotoxic effect studies on cortex neuron cells and neuroblastoma SH-SY5Y cell line were especially determined compounds **6a**, **6d**, and **6h** be orally bioavailable, highly potent, and brain penetrant AChEIs and *h*CAIs. These favorable outcomes motivate us to detect further therapeutic values; more efforts for discovering novel multi-target AChEIs and *h*CAIs are currently underway.

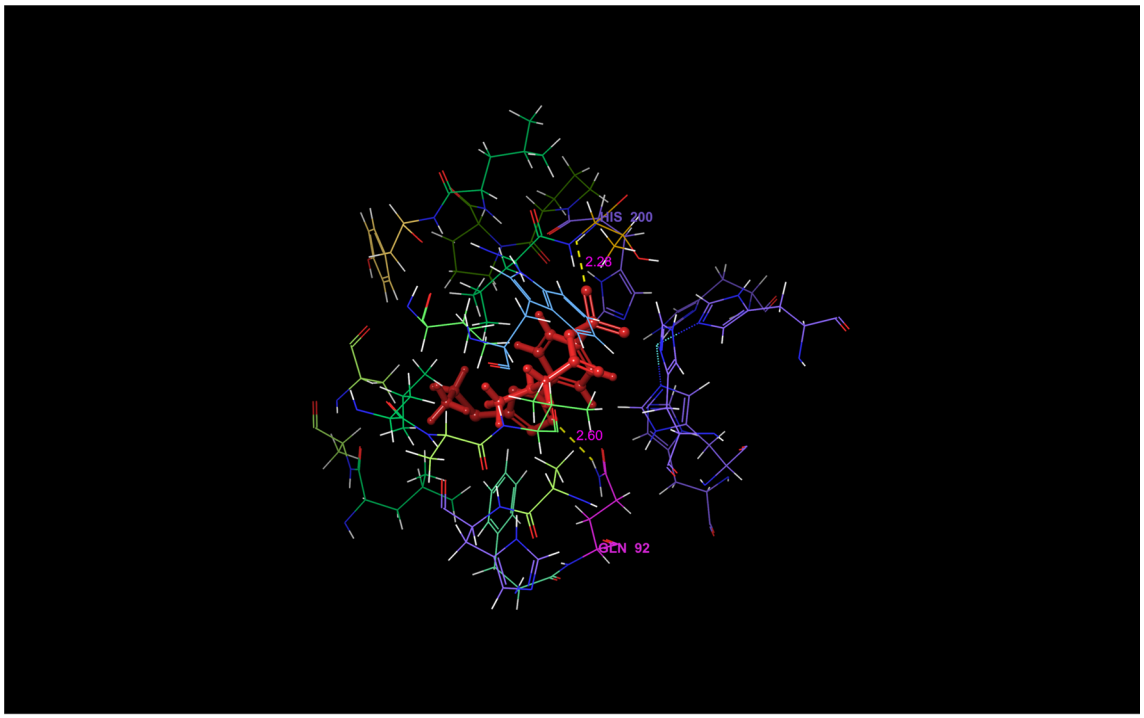


(A)

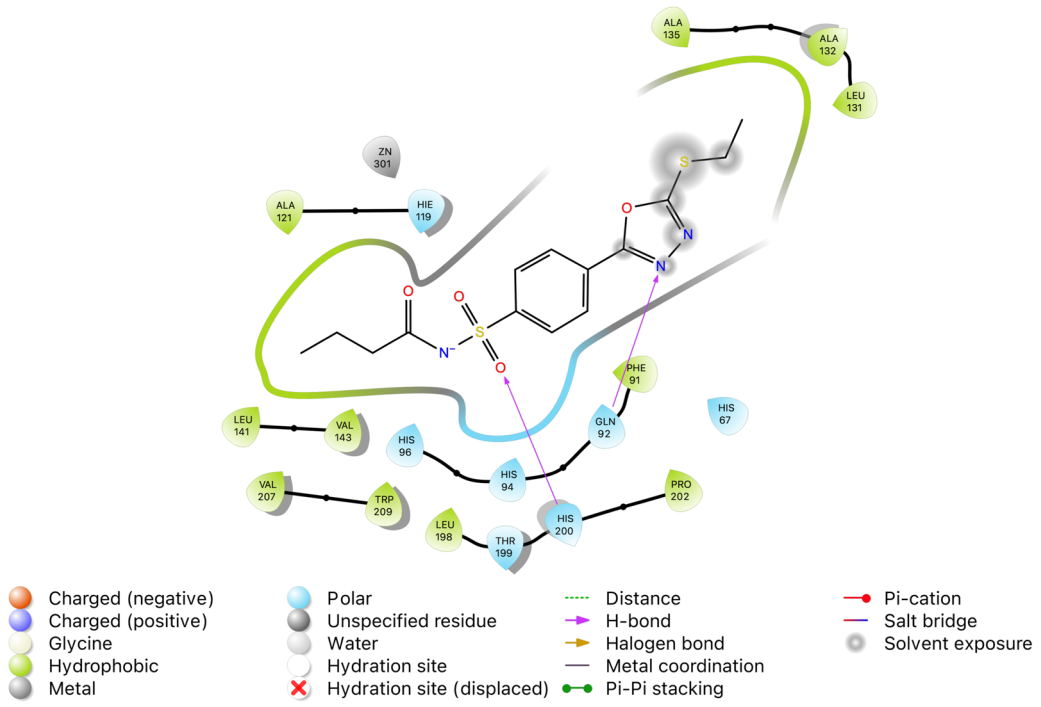


(B)

Fig. 5 **A** 3D interaction of the derivative **6h** ($C_{18}H_{25}N_3O_4S_2$: *N*-([4-(5-(ethylthio)-1,3,4-oxadiazol-2-yl)phenyl]sulfonyl)octanamide) with the key amino acids within the active site of AChE (PDB iD: 4EY7). **B** 2D docking pose of the derivative **6h** ($C_{18}H_{25}N_3O_4S_2$: *N*-([4-(5-(ethylthio)-1,3,4-oxadiazol-2-yl)phenyl]sulfonyl)octanamide) with the key amino acids within the binding site of AChE (PDB iD: 4EY7)

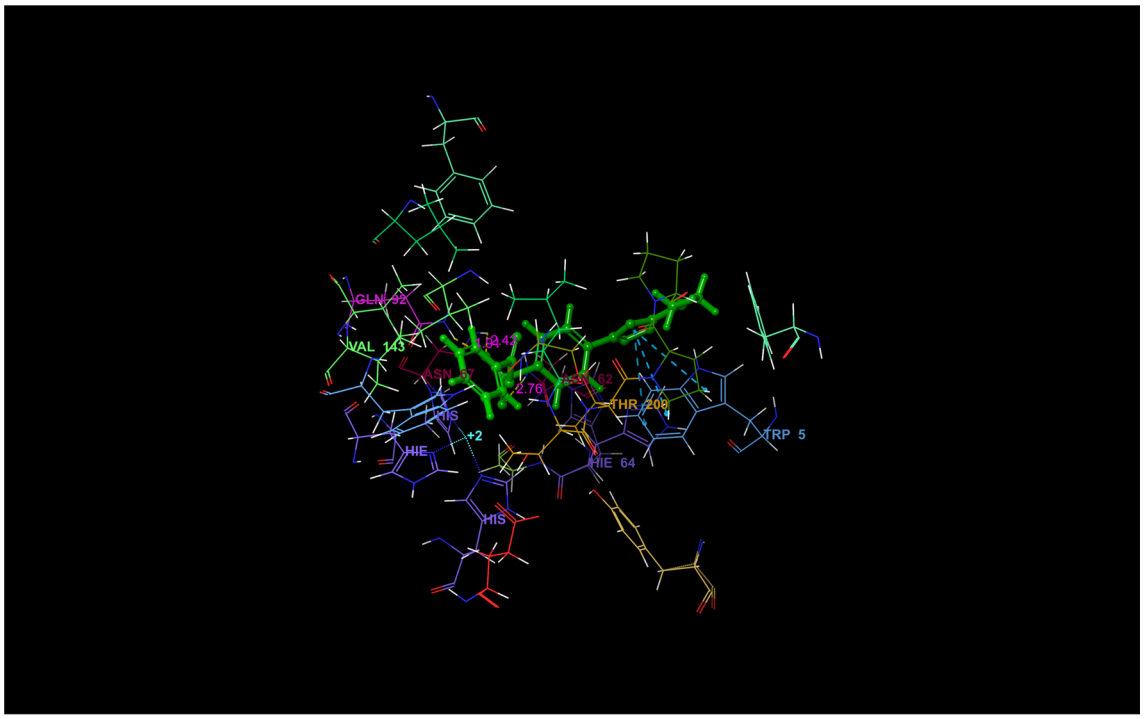


(A)

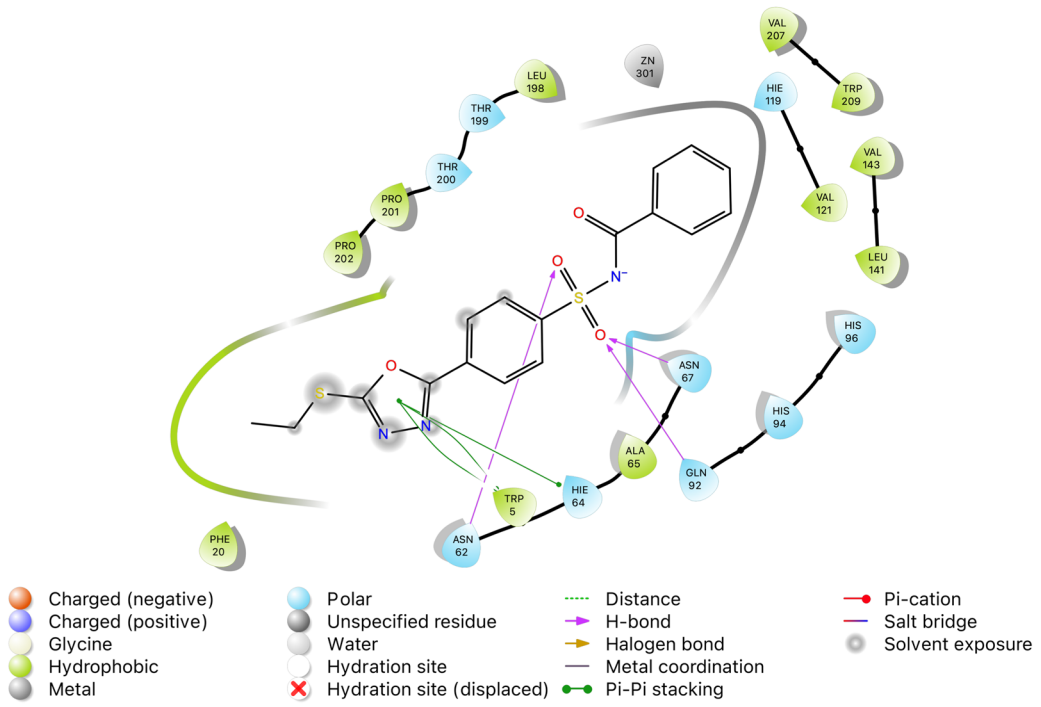


(B)

Fig. 6 **A** 3D interaction of the derivative **6d** ($C_{14}H_{17}N_3O_4S_2$: *N*-([4-(5-(ethylthio)-1,3,4-oxadiazol-2-yl)phenyl]sulfonyl)butyramide) with the key amino acids within the active site of *h*CA I (PDB iD: 6I0L). **B** 2D docking pose of the derivative **6d** ($C_{14}H_{17}N_3O_4S_2$: *N*-([4-(5-(ethylthio)-1,3,4-oxadiazol-2-yl)phenyl]sulfonyl)butyramide) with the key amino acids within the binding site of *h*CA I (PDB iD: 6I0L)



(A)



(B)

Fig. 7 **A** 3D interaction of the derivative **6a** ($C_{17}H_{15}N_3O_4S_2$: *N*-([4-(5-(ethylthio)-1,3,4-oxadiazol-2-yl)phenyl]sulfonyl)benzamide) with the key amino acids within the active site of *h*CA II (PDB iD: 5NY3). **B** 2D docking pose of the derivative **6a** ($C_{17}H_{15}N_3O_4S_2$: *N*-([4-(5-(ethylthio)-1,3,4-oxadiazol-2-yl)phenyl]sulfonyl)benzamide) with the key amino acids within the binding site of *h*CA II (PDB iD: 5NY3)

Supplementary Information The online version contains supplementary material available at https://doi.org/10.1007/s11030-022-10422-8.

Acknowledgements This work was supported by the Research Fund of Erzincan Binali Yıldırım University (Grant Number TSA-2020-729) and the Research Fund of Anadolu University (Grant Number 2102S003).

Declarations

Conflict of interest The authors declare that there is no conflict of interest.

References

1. Li JJ (2013) Heterocyclic chemistry in drug discovery. John Wiley & Sons
2. Tripathi AC, Gupta SJ, Fatima GN, Sonar PK, Verma A, Saraf SK (2014) 4-Thiazolidinones: the advances continue…. Eur J Med Chem. https://doi.org/10.1016/j.ejmech.2013.11.017
3. Bhat MA (2014) Synthesis and anti-mycobacterial activity of new 4-thiazolidinone and 1,3,4-oxadiazole derivatives of isoniazid. Acta Pol Pharm 71(5):763–770
4. Szychowski KA, Leja ML, Kaminskyy DV, Binduga UE, Pinyazhko R, Lesyk RB et al (2017) Study of novel anticancer 4-thiazolidinone derivatives. Chem-Biol Interact. https://doi.org/10.1016/j.cbi.2016.12.008
5. Suryawanshi R, Jadhav S, Makwana N, Desai D, Chaturbhuj D, Sonawani A et al (2017) Evaluation of 4-thiazolidinone derivatives as potential reverse transcriptase inhibitors against HIV-1 drug resistant strains. Bioorg Chem. https://doi.org/10.1016/j.bioorg.2017.02.007
6. Deep A, Jain S, Sharma PC, Mittal SK, Phogat P, Malhotra M (2014) Synthesis, characterization and antimicrobial evaluation of 2, 5-disubstituted-4-thiazolidinone derivatives. Arabian J Chem 7(3):287–291. https://doi.org/10.1016/j.arabjc.2010.10.032
7. Kunzler A, Neuenfeldt PD, das Neves AM, Pereira CM, Marques GH, Nascente PS et al (2013) Synthesis, antifungal and cytotoxic activities of 2-aryl-3-((piperidin-1-yl) ethyl) thiazolidinones. Eur J Med Chem. https://doi.org/10.1016/j.ejmech.2013.03.030
8. Derawey SH, Mosa MN, Jasim EQ, Hraishawi RM (2019) Synthesis, characterization and antibacterial evaluation of 1,3,4-oxadiazole derivatives. Int J Res Pharm Sci 10(3):2342–2350
9. Nayak SG, Poojary B (2019) A review on the preparation of 1,3,4-oxadiazoles from the dehydration of hydrazines and study of their biological roles. Chem Afr. https://doi.org/10.1007/s42250-019-00084-9
10. Dholaria P, Parikh K, Joshi D, Joshi A (2018) Synthesis, characterization and antimicrobial screening of sulphonamide based 1, 3, 4-oxadiazoles. Int J Chem Phys Sci 7(2):13. https://doi.org/10.30731/ijcps.7.2.2018.13-26
11. Boström J, Hogner A, Llinàs A, Wellner E, Plowright AT (2012) Oxadiazoles in medicinal chemistry. J Med Chem 55(5):1817–1830. https://doi.org/10.1021/jm2013248
12. Savarino A (2006) A historical sketch of the discovery and development of HIV-1 integrase inhibitors. Expert Opin Invest Drugs 15(12):1507–1522. https://doi.org/10.1517/13543784.15.12.1507
13. James ND, Growcott JW (2009) Zibotentan endothelin ETA receptor antagonist oncolytic. Drugs Future 34(8):624–633. https://doi.org/10.1358/dof.2009.34.8.1400202
14. Ogata M, Atobe H, Kushida H, Yamamoto K (1971) In vitro sensitivity of mycoplasmas isolated from various animals and sewage to antibiotics and nitrofurans. J Antibiotics 24(7):443–451. https://doi.org/10.7164/antibiotics.24.443
15. Vardan S, Smulyan H, Mookherjee S, Eich R (1983) Effects of tiodazosin, a new antihypertensive, hemodynamics and clinical variables. Clin Pharmacol Ther 34(3):290–296. https://doi.org/10.1038/clpt.1983.170
16. Krzywik J, Mozga W, Aminpour M, Janczak J, Maj E, Wietrzyk J et al (2020) Synthesis, antiproliferative activity and molecular docking studies of novel doubly modified colchicine amides and sulfonamides as anticancer agents. Molecules 25(8):1789. https://doi.org/10.3390/molecules25081789
17. El-Sayed NS, El-Bendary ER, El-Ashry SM, El-Kerdawy MM (2011) Synthesis and antitumor activity of new sulfonamide derivatives of thiadiazolo [3, 2-a] pyrimidines. Eur J Med Chem 46(9):3714–3720. https://doi.org/10.1016/j.ejmech.2011.05.037
18. Johansson A, Poliakov A, Åkerblom E, Wiklund K, Lindeberg G, Winiwarter S et al (2003) Acyl sulfonamides as potent protease inhibitors of the hepatitis C virus full-length NS3 (protease-helicase/NTPase): a comparative study of different C-terminals. Bioorg Med Chem 11(12):2551–2568. https://doi.org/10.1016/S0968-0896(03)00179-2
19. Galal AM, Fayad W, Mettwally WS, Gomaa SK, Ahmed ER, El-Refai HA et al (2019) Cytotoxicity of multicellular cancer spheroids, antibacterial, and antifungal of selected sulfonamide derivatives coupled with a salicylamide and/or anisamide scaffold. Med Chem Res 28(9):1425–1440. https://doi.org/10.1007/s00044-019-02382-w
20. Bano S, Javed K, Ahmad S, Rathish I, Singh S, Alam M (2011) Synthesis and biological evaluation of some new 2-pyrazolines bearing benzene sulfonamide moiety as potential anti-inflammatory and anti-cancer agents. Eur J Med Chem 46(12):5763–5768. https://doi.org/10.1016/j.ejmech.2011.08.015
21. Li J, Lou J, Wang Z, Wang T, Xiao Y, Xianming H, Liu P, Hong X (2015) Design, synthesis and pharmacological evaluation of novel *N*-(2-(1, 1-dimethyl-5, 7-dioxo-4, 6-diazaspiro[2.4]heptan-6-yl)ethyl) sulfonamide derivatives as potential anticonvulsant agents. Eur J Med Chem 92:370–376. https://doi.org/10.1016/j.ejmech.2015.01.008
22. Richey DP, Brown GM (1969) The biosynthesis of folic acid IX. Purification and properties of the enzymes required for the formation of dihydropteroic acid. J Biol Chem 244(6):1582–1592
23. Brown GM (1962) The biosynthesis of folic acid. J Biol Chem 237(2):536–540. https://doi.org/10.1016/S0021-9258(18)93957-8
24. Sahoo J, Kshiroda P, Sarangi N, Rout S, Paidesetty S (2020) In silico investigation and biological evaluation of synthesized sulfamethoxazole derivatives. Indian J Pharm Sci 82(1):123–130
25. Nasr T, Bondock S, Eid S (2014) Design, synthesis, antimicrobial evaluation and molecular docking studies of some new thiophene, pyrazole and pyridone derivatives bearing sulfisoxazole moiety. Eur J Med Chem. https://doi.org/10.1016/j.ejmech.2014.07.052
26. Lv Y, Xu J, Xu K, Liu X, Guo X, Lu S et al (2020) Accumulation characteristics and biological response of ginger to sulfamethoxazole and ofloxacin. Environ Pollut. https://doi.org/10.1016/j.envpol.2020.114203
27. Durgun M, Türkeş C, Işık M, Demir Y, Saklı A, Kuru A et al (2020) Synthesis, characterization, biological evaluation and in silico studies of sulfonamide Schiff bases. J Enzyme Inhib Med Chem 35(1):950–962. https://doi.org/10.1080/14756366.2020.1746784
28. Taslimi P, Işık M, Türkan F, Durgun M, Türkeş C, Gülçin İ et al (2020) Benzenesulfonamide derivatives as potent acetylcholinesterase, α-glycosidase, and glutathione S-transferase

inhibitors: biological evaluation and molecular docking studies. J Biomol Struct Dyn. https://doi.org/10.1080/07391102.2020.1790422
29. Scheidt KA, Roush WR, McKerrow JH, Selzer PM, Hansell E, Rosenthal PJ (1998) Structure-based design, synthesis and evaluation of conformationally constrained cysteine protease inhibitors. Bioorg Med Chem 6(12):2477–2494. https://doi.org/10.1016/S0968-0896(98)80022-9
30. Yamali C, Gül Hİ, Demir Y, Kazaz C, Gülçin İ (2020) Synthesis and bioactivities of 1-(4-hydroxyphenyl)-2-((heteroaryl) thio) ethanones as carbonic anhydrase I, II and acetylcholinesterase inhibitors. Turk J Chem 44(4):1058–1067. https://doi.org/10.3906/kim-2004-36
31. Akocak S, Taslimi P, Lolak N, Işık M, Durgun M, Budak Y et al (2021) Synthesis, characterization, and inhibition study of novel substituted phenylureido sulfaguanidine derivatives as α-glycosidase and cholinesterase inhibitors. Chem Biodivers 18(4):e2000958. https://doi.org/10.1002/cbdv.202000958
32. Kalaycı M, Türkeş C, Arslan M, Demir Y, Beydemir Ş (2020) Novel benzoic acid derivatives: synthesis and biological evaluation as multi-target acetylcholinesterase and carbonic anhydrase inhibitors. Arch Pharm 354(3):e2000282. https://doi.org/10.1002/ardp.202000282
33. Aydin BO, Anil D, Demir Y (2021) Synthesis of N-alkylated pyrazolo[3,4-d] pyrimidine analogs and evaluation of acetylcholinesterase and carbonic anhydrase inhibition properties. Arch Pharm 354(5):2000330. https://doi.org/10.1002/ardp.202000330
34. Turkan F, Çetin A, Taslimi P, Karaman M, Gulçin İ (2019) Synthesis, biological evaluation and molecular docking of novel pyrazole derivatives as potent carbonic anhydrase and acetylcholinesterase inhibitors. Bioorg Chem. https://doi.org/10.1016/j.bioorg.2019.02.013
35. Sever B, Türkeş C, Altıntop MD, Demir Y, Beydemir Ş (2020) Thiazolyl-pyrazoline derivatives: in vitro and in silico evaluation as potential acetylcholinesterase and carbonic anhydrase inhibitors. Int J Biol Macromol. https://doi.org/10.1016/j.ijbiomac.2020.09.043
36. Türkeş C, Demir Y, Beydemir Ş (2021) Calcium channel blockers: molecular docking and inhibition studies on carbonic anhydrase I and II isoenzymes. J Biomol Struct Dyn 39(5):1672–1680. https://doi.org/10.1080/07391102.2020.1736631
37. Tugrak M, Gul HI, Demir Y, Gulcin I (2020) Synthesis of benzamide derivatives with thiourea-substituted benzenesulfonamides as carbonic anhydrase inhibitors. Arch Pharm 354(2):e2000230. https://doi.org/10.1002/ardp.202000230
38. Istrefi Q, Türkeş C, Arslan M, Demir Y, Nixha AR, Beydemir Ş et al (2020) Sulfonamides incorporating ketene *N*,*S*-acetal bioisosteres as potent carbonic anhydrase and acetylcholinesterase inhibitors. Arch Pharm 353(6):e1900383. https://doi.org/10.1002/ardp.201900383
39. Hoff E, Zou D, Schiza S, Demir Y, Grote L, Bouloukaki I et al (2020) Carbonic anhydrase, obstructive sleep apnea and hypertension: effects of intervention. J Sleep Res 29(2):e12956. https://doi.org/10.1111/jsr.12956
40. Türkeş C, Arslan M, Demir Y, Cocaj L, Nixha AR, Beydemir Ş (2019) Synthesis, biological evaluation and in silico studies of novel N-substituted phthalazine sulfonamide compounds as potent carbonic anhydrase and acetylcholinesterase inhibitors. Bioorg Chem. https://doi.org/10.1016/j.bioorg.2019.103004
41. Bilginer S, Gul HI, Anil B, Demir Y, Gulcin I (2021) Synthesis and in silico studies of triazene-substituted sulfamerazine derivatives as acetylcholinesterase and carbonic anhydrases inhibitors. Arch Pharm 354(1):2000243. https://doi.org/10.1002/ardp.202000243
42. Ellman GL, Courtney KD, Andres V Jr, Featherstone RM (1961) A new and rapid colorimetric determination of acetylcholinesterase activity. Biochem Pharmacol 7(2):88–95. https://doi.org/10.1016/0006-2952(61)90145-9
43. Topal M (2019) The inhibition profile of sesamol against α-glycosidase and acetylcholinesterase enzymes. Int J Food Prop 22(1):1527–1535. https://doi.org/10.1080/10942912.2019.1656234
44. Yamali C, Gul HI, Cakir T, Demir Y, Gulcin I (2020) Aminoalkylated phenolic chalcones: investigation of biological effects on acetylcholinesterase and carbonic anhydrase I and II as potential lead enzyme inhibitors. Lett Drug Des Discov 17(10):1283–1292. https://doi.org/10.2174/1570180817999200520123510
45. Askin S, Tahtaci H, Türkeş C, Demir Y, Ece A, Çiftçi GA et al (2021) Design, synthesis, characterization, in vitro and in silico evaluation of novel imidazo [2, 1-b][1, 3, 4] thiadiazoles as highly potent acetylcholinesterase and non-classical carbonic anhydrase inhibitors. Bioorg Chem. https://doi.org/10.1016/j.bioorg.2021.105009
46. Verpoorte JA, Mehta S, Edsall JT (1967) Esterase activities of human carbonic anhydrases B and C. J Biol Chem 242(18):4221–4229. https://doi.org/10.1016/S0021-9258(18)95800-X
47. Topal F (2019) Inhibition profiles of voriconazole against acetylcholinesterase, α-glycosidase, and human carbonic anhydrase I and II isoenzymes. J Biochem Mol Toxicol 33(10):e22385. https://doi.org/10.1002/jbt.22385
48. Caglayan C, Gulcin İ (2018) The toxicological effects of some avermectins on goat liver carbonic anhydrase enzyme. J Biochem Mol Toxicol 32(1):e22010. https://doi.org/10.1002/jbt.22010
49. Johnson KA, Goody RS (2011) The original Michaelis constant: translation of the 1913 Michaelis–Menten paper. Biochemistry 50(39):8264–8269. https://doi.org/10.1021/bi201284u
50. Türkeş C, Kesebir Öztürk A, Demir Y, Küfrevioğlu Öİ, Beydemir Ş (2021) Calcium channel blockers: the effect of glutathione S-transferase enzyme activity and molecular docking studies. ChemistrySelect 6(40):11137–11143. https://doi.org/10.1002/slct.202103100
51. Tokalı FS, Demir Y, Demircioğlu İH, Türkeş C, Kalay E, Şendil K et al (2021) Synthesis, biological evaluation, and in silico study of novel library sulfonates containing quinazolin-4 (3H)-one derivatives as potential aldose reductase inhibitors. Drug Dev Res. https://doi.org/10.1002/ddr.21887
52. Lineweaver H, Burk D (1934) The determination of enzyme dissociation constants. J Am Chem Soc 56(3):658–666. https://doi.org/10.1021/ja01318a036
53. Demir Y (2020) Naphthoquinones, benzoquinones, and anthraquinones: Molecular docking, ADME and inhibition studies on human serum paraoxonase-1 associated with cardiovascular diseases. Drug Dev Res 81(5):628–636. https://doi.org/10.1002/ddr.21667
54. Çalışkan B, Kesebir AÖ, Demir Y, Salman İA (2021) The effect of brimonidine and proparacaine on metabolic enzymes: glucose-6-phosphate dehydrogenase, 6-phosphogluconate dehydrogenase, and glutathione reductase. Biotechnol Appl Biochem 69(1):281–288. https://doi.org/10.1002/bab.2107
55. Türkeş C, Söyüt H, Beydemir Ş (2014) Effect of calcium channel blockers on paraoxonase-1 (PON1) activity and oxidative stress. Pharmacol Rep 66(1):74–80. https://doi.org/10.1016/j.pharep.2013.08.007
56. Türkeş C, Söyüt H, Beydemir Ş (2015) Human serum paraoxonase-1 (hPON1): in vitro inhibition effects of moxifloxacin hydrochloride, levofloxacin hemihidrate, cefepime hydrochloride, cefotaxime sodium and ceftizoxime sodium. J Enzyme Inhib Med Chem 30(4):622–628. https://doi.org/10.3109/14756366.2014.959511
57. Türkeş C, Söyüt H, Beydemir Ş (2016) In vitro inhibitory effects of palonosetron hydrochloride, bevacizumab and

cyclophosphamide on purified paraoxonase-I (hPON1) from human serum. Environ Toxicol Pharmacol. https://doi.org/10.1016/j.etap.2015.11.024
58. Akbaba Y, Türkeş C, Polat L, Söyüt H, Şahin E, Menzek A et al (2013) Synthesis and paroxonase activities of novel bromophenols. J Enzyme Inhib Med Chem 28(5):1073–1079. https://doi.org/10.3109/14756366.2012.715287
59. Türkeş C, Demir Y, Beydemir Ş (2019) Anti-diabetic properties of calcium channel blockers: inhibition effects on aldose reductase enzyme activity. Appl Biochem Biotechnol 189(1):318–329. https://doi.org/10.1007/s12010-019-03009-x
60. Demir Y (2019) The behaviour of some antihypertension drugs on human serum paraoxonase-1: an important protector enzyme against atherosclerosis. J Pharm Pharmacol 71(10):1576–1583. https://doi.org/10.1111/jphp.13144
61. Hasbullah N, Mazatulikhma MZ, Kamarulzaman N (2013) Nanotoxicity of magnesium oxide on human neuroblastoma SH-SY5Y cell lines. Advanced Materials Research. Trans Tech Publ, pp 160–164
62. Valencia ME, Herrera-Arozamena C, de Andrés L, Pérez C, Morales-García JA, Pérez-Castillo A et al (2018) Neurogenic and neuroprotective donepezil-flavonoid hybrids with sigma-1 affinity and inhibition of key enzymes in Alzheimer's disease. Eur J Med Chem. https://doi.org/10.1016/j.ejmech.2018.07.026
63. Taghizadehghalehjoughi A, Sezen S, Hacimuftuoglu A, Güllüce M (2019) Vincristine combination with Ca+ 2 channel blocker increase antitumor effects. Mol Biol Rep 46(2):2523–2528. https://doi.org/10.1007/s11033-019-04706-w
64. Ertugrul MS, Nadaroglu H, Nalci OB, Hacimuftuoglu A, Alayli A (2020) Preparation of CoS nanoparticles-cisplatin bio-conjugates and investigation of their effects on SH-SY5Y neuroblastoma cell line. Cytotechnology 72(6):885–896. https://doi.org/10.1007/s10616-020-00432-5
65. Nalci OB, Nadaroglu H, Genc S, Hacimuftuoglu A, Alayli A (2020) The effects of MgS nanoparticles-Cisplatin-bio-conjugate on SH-SY5Y neuroblastoma cell line. Mol Biol Rep 47(12):9715–9723. https://doi.org/10.1007/s11033-020-05987-2
66. Wright WC, Chenge J, Wang J, Girvan HM, Yang L, Chai SC et al (2020) Clobetasol propionate is a heme-mediated selective inhibitor of human cytochrome P450 3A5. J Med Chem 63(3):1415–1433. https://doi.org/10.1021/acs.jmedchem.9b02067
67. Türkeş C (2019) Investigation of potential paraoxonase-I inhibitors by kinetic and molecular docking studies: chemotherapeutic drugs. Protein Pept Lett 26(6):392–402. https://doi.org/10.2174/0929866526666190226162225
68. Işık M, Beydemir Ş, Demir Y, Durgun M, Türkeş C, Nasır A et al (2020) Benzenesulfonamide derivatives containing imine and amine groups: inhibition on human paraoxonase and molecular docking studies. Int J Biol Macromol. https://doi.org/10.1016/j.ijbiomac.2019.09.237
69. Işık M, Akocak S, Lolak N, Taslimi P, Türkeş C, Gülçin İ et al (2020) Synthesis, characterization, biological evaluation, and in silico studies of novel 1,3-diaryltriazene-substituted sulfathiazole derivatives. Arch Pharm 353(9):e2000102. https://doi.org/10.1002/ardp.202000102
70. Türkeş C, Demir Y, Beydemir Ş (2022) Some calcium-channel blockers: kinetic and in silico studies on paraoxonase-I. J Biomol Struct Dyn 40(1):77–85. https://doi.org/10.1080/07391102.2020.1806927
71. Lipinski CA, Lombardo F, Dominy BW, Feeney PJ (1997) Experimental and computational approaches to estimate solubility and permeability in drug discovery and development settings. Adv Drug Deliv Rev 23(1–3):3–25. https://doi.org/10.1016/S0169-409X(96)00423-1
72. Duffy EM, Jorgensen WL (2000) Prediction of properties from simulations: free energies of solvation in hexadecane, octanol, and water. J Am Chem Soc 122(12):2878–2888. https://doi.org/10.1021/ja993663t
73. Baell JB, Holloway GA (2010) New substructure filters for removal of pan assay interference compounds (PAINS) from screening libraries and for their exclusion in bioassays. J Med Chem 53(7):2719–2740. https://doi.org/10.1021/jm901137j
74. Türkeş C (2019) A potential risk factor for paraoxonase 1: in silico and in-vitro analysis of the biological activity of proton-pump inhibitors. J Pharm Pharmacol 71(10):1553–1564. https://doi.org/10.1111/jphp.13141
75. Beydemir Ş, Türkeş C, Yalçın A (2021) Gadolinium-based contrast agents: in vitro paraoxonase 1 inhibition, in silico studies. Drug Chem Toxicol 44(5):508–517. https://doi.org/10.1080/01480545.2019.1620266
76. Işık M, Demir Y, Durgun M, Türkeş C, Necip A, Beydemir Ş (2020) Molecular docking and investigation of 4-(benzylideneamino)-and 4-(benzylamino)-benzenesulfonamide derivatives as potent AChE inhibitors. Chem Pap. https://doi.org/10.1007/s11696-019-00988-3
77. Kilic A, Beyazsakal L, Işık M, Türkeş C, Necip A, Takım K et al (2020) Mannich reaction derived novel boron complexes with amine-bis(phenolate) ligands: synthesis, spectroscopy and in vitro/in silico biological studies. J Organomet Chem. https://doi.org/10.1016/j.jorganchem.2020.121542
78. Gündoğdu S, Türkeş C, Arslan M, Demir Y, Beydemir Ş (2019) New Isoindole-1, 3-dione substituted sulfonamides as potent inhibitors of carbonic anhydrase and acetylcholinesterase: design, synthesis, and biological evaluation. ChemistrySelect 4(45):13347–13355. https://doi.org/10.1002/slct.201903458
79. Sever B, Altıntop MD, Demir Y, Türkeş C, Özbaş K, Çiftçi GA et al (2021) A new series of 2,4-thiazolidinediones endowed with potent aldose reductase inhibitory activity. Open Chem. https://doi.org/10.1515/chem-2021-0032
80. Cheung J, Rudolph MJ, Burshteyn F, Cassidy MS, Gary EN, Love J et al (2012) Structures of human acetylcholinesterase in complex with pharmacologically important ligands. J Med Chem 55(22):10282–10286. https://doi.org/10.1021/jm300871x
81. Bozdag M, Ferraroni M, Ward C, Carta F, Bua S, Angeli A et al (2019) Carbonic anhydrase inhibitors based on sorafenib scaffold: design, synthesis, crystallographic investigation and effects on primary breast cancer cells. Eur J Med Chem. https://doi.org/10.1016/j.ejmech.2019.111600
82. Pecina A, Brynda J, Vrzal L, Gnanasekaran R, Hořejší M, Eyrilmez SM et al (2018) Ranking power of the SQM/COSMO scoring function on carbonic anhydrase II–inhibitor complexes. ChemPhysChem 19(7):873–879. https://doi.org/10.1002/cphc.201701104
83. Türkeş C, Beydemir Ş, Küfrevioğlu Öİ (2019) In vitro and in silico studies on the toxic effects of antibacterial drugs as human serum paraoxonase 1 inhibitor. ChemistrySelect 4(33):9731–9736. https://doi.org/10.1002/slct.201902424
84. Sastry GM, Adzhigirey M, Day T, Annabhimoju R, Sherman W (2013) Protein and ligand preparation: parameters, protocols, and influence on virtual screening enrichments. J Comput-Aided Mol Des 27(3):221–234. https://doi.org/10.1007/s10822-013-9644-8
85. Demir Y, Ceylan H, Türkeş C, Beydemir Ş (2021) Molecular docking and inhibition studies of vulpinic, carnosic and usnic acids on polyol pathway enzymes. J Biomol Struct Dyn. https://doi.org/10.1080/07391102.2021.1967195
86. Türkeş C, Beydemir Ş (2020) Inhibition of human serum paraoxonase-I with antimycotic drugs: in vitro and in silico studies. Appl Biochem Biotechnol 190(1):252–269. https://doi.org/10.1007/s12010-019-03073-3

87. Halgren TA (2009) Identifying and characterizing binding sites and assessing druggability. J Chem Inf Model 49(2):377–389. https://doi.org/10.1021/ci800324m
88. Lolak N, Akocak S, Türkeş C, Taslimi P, Işık M, Beydemir Ş et al (2020) Synthesis, characterization, inhibition effects, and molecular docking studies as acetylcholinesterase, α-glycosidase, and carbonic anhydrase inhibitors of novel benzenesulfonamides incorporating 1,3,5-triazine structural motifs. Bioorg Chem. https://doi.org/10.1016/j.bioorg.2020.103897
89. Sever B, Türkeş C, Altıntop MD, Demir Y, Çiftçi GA, Beydemir Ş (2021) Novel metabolic enzyme inhibitors designed through the molecular hybridization of thiazole and pyrazoline scaffolds. Arch Pharm 354(12):e2100294. https://doi.org/10.1002/ardp.202100294
90. Friesner RA, Murphy RB, Repasky MP, Frye LL, Greenwood JR, Halgren TA et al (2006) Extra precision glide: docking and scoring incorporating a model of hydrophobic enclosure for protein−ligand complexes. J Med Chem 49(21):6177–6196. https://doi.org/10.1021/jm051256o
91. Demir Y, Türkeş C, Beydemir Ş (2020) Molecular docking studies and inhibition properties of some antineoplastic agents against paraoxonase-I. Anti-Cancer Agents Med Chem 20(7):887–896. https://doi.org/10.2174/1871520620666200218110645
92. Ece A (2020) Towards more effective acetylcholinesterase inhibitors: a comprehensive modelling study based on human acetylcholinesterase protein–drug complex. J Biomol Struct Dyn 38(2):565–572. https://doi.org/10.1080/07391102.2019.1583606
93. Barreiro G, Guimarães CR, Tubert-Brohman I, Lyons TM, Tirado-Rives J, Jorgensen WL (2007) Search for non-nucleoside inhibitors of HIV-1 reverse transcriptase using chemical similarity, molecular docking, and MM-GB/SA scoring. J Chem Inf Model 47(6):2416–2428. https://doi.org/10.1021/ci700271z
94. Yaşar Ü, Gönül İ, Türkeş C, Demir Y, Beydemir Ş (2021) Transition-metal complexes of bidentate Schiff-base ligands: in vitro and in silico evaluation as non-classical carbonic anhydrase and potential acetylcholinesterase inhibitors. ChemistrySelect 29(6):7278–7284. https://doi.org/10.1002/slct.202102082
95. Türkeş C, Akocak S, Işık M, Lolak N, Taslimi P, Durgun M et al (2021) Novel inhibitors with sulfamethazine backbone: synthesis and biological study of multi-target cholinesterases and α-glucosidase inhibitors. J Biomol Struct Dyn. https://doi.org/10.1080/07391102.2021.1916599
96. Türkeş C, Demir Y, Beydemir Ş (2021) Infection medications: assessment In-vitro glutathione S-transferase inhibition and molecular docking study. ChemistrySelect 6(43):11915–11924. https://doi.org/10.1002/slct.202103197
97. Çalışkan B, Demir Y, Türkeş C (2021) Ophthalmic drugs: in vitro paraoxonase 1 inhibition and molecular docking studies. Biotechnol Appl Biochem. https://doi.org/10.1002/bab.2284
98. Kılıcaslan S, Arslan M, Ruya Z, Bilen Ç, Ergün A, Gençer N et al (2016) Synthesis and evaluation of sulfonamide-bearing thiazole as carbonic anhydrase isoforms hCA I and hCA II. J Enzyme Inhib Med Chem 31(6):1300–1305. https://doi.org/10.3109/14756366.2015.1128426
99. Sharma V, Kumar R, Angeli A, Supuran CT, Sharma PK (2020) Tail approach synthesis of novel benzenesulfonamides incorporating 1, 3, 4-oxadiazole hybrids as potent inhibitor of carbonic anhydrase I, II, IX, and XII isoenzymes. Eur J Med Chem. https://doi.org/10.1016/j.ejmech.2020.112219
100. Rutkauskas K, Zubrienė A, Tumosienė I, Kantminienė K, Kažemėkaitė M, Smirnov A et al (2014) 4-amino-substituted benzenesulfonamides as inhibitors of human carbonic anhydrases. Molecules 19(11):17356–17380. https://doi.org/10.3390/molecules191117356
101. Xie H-r, Hu L-s, Li G-y (2010) SH-SY5Y human neuroblastoma cell line: in vitro cell model of dopaminergic neurons in Parkinson's disease. Chinese Med J 123(8):1086–1092. https://doi.org/10.3760/cma.j.issn.0366-6999.2010.08.021

Publisher's Note Springer Nature remains neutral with regard to jurisdictional claims in published maps and institutional affiliations.

Authors and Affiliations

Özcan Güleç[1] · Cüneyt Türkeş[2] · Mustafa Arslan[1] · Yeliz Demir[3] · Yeşim Yeni[4] · Ahmet Hacımüftüoğlu[4] · Ergün Ereminsoy[5] · Ömer İrfan Küfrevioğlu[5] · Şükrü Beydemir[6,7]

✉ Cüneyt Türkeş
cuneyt.turkes@erzincan.edu.tr

✉ Mustafa Arslan
marslan@sakarya.edu.tr

[1] Department of Chemistry, Faculty of Arts and Science, Sakarya University, 54187 Serdivan, Sakarya, Türkiye

[2] Department of Biochemistry, Faculty of Pharmacy, Erzincan Binali Yıldırım University, 24002 Erzincan, Türkiye

[3] Department of Pharmacy Services, Nihat Delibalta Göle Vocational High School, Ardahan University, 75700 Ardahan, Türkiye

[4] Department of Medical Pharmacology, Faculty of Medicine, Atatürk University, 25240 Erzurum, Türkiye

[5] Department of Chemistry, Faculty of Science, Atatürk University, 25240 Erzurum, Türkiye

[6] Department of Biochemistry, Faculty of Pharmacy, Anadolu University, 26470 Eskişehir, Türkiye

[7] The Rectorate of Bilecik Şeyh Edebali University, 11230 Bilecik, Türkiye